Article

Rhodium Boryl Complexes in the Catalytic, Terminal Functionalization of Alkanes

John F. Hartwig, Kevin S. Cook, Marko Hapke, Christopher D. Incarvito, Yubo Fan, Charles Edwin Webster, and Michael B. Hall

J. Am. Chem. Soc., **2005**, 127 (8), 2538-2552• DOI: 10.1021/ja045090c • Publication Date (Web): 03 February 2005

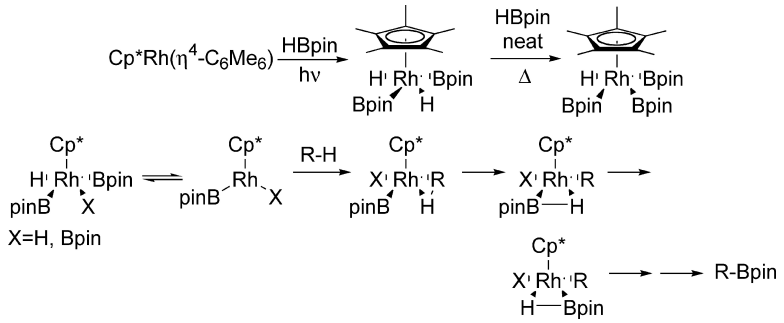

More About This Article

Additional resources and features associated with this article are available within the HTML version:

- Supporting Information
- Links to the 26 articles that cite this article, as of the time of this article download
- Access to high resolution figures
- Links to articles and content related to this article
- Copyright permission to reproduce figures and/or text from this article

View the Full Text HTML

J|A|C|S
ARTICLES
Published on Web 02/03/2005

Rhodium Boryl Complexes in the Catalytic, Terminal Functionalization of Alkanes

John F. Hartwig,*,† Kevin S. Cook,† Marko Hapke,† Christopher D. Incarvito,† Yubo Fan,‡ Charles Edwin Webster,‡ and Michael B. Hall*,‡

Contribution from the Departments of Chemistry, Yale University, P.O. Box 208107, New Haven, Connecticut 06520-8107, and Texas A&M University, College Station, Texas 77843-3255

Received August 15, 2004; E-mail: john.hartwig@yale.edu

Abstract: A series of studies have been conducted by experimental and theoretical methods on the synthesis, structures, and reactions of Cp*Rh boryl complexes that are likely intermediates in the rhodium-catalyzed regioselective, terminal functionalization of alkanes. The photochemical reaction of Cp*Rh(η^6-C_6Me_6) with pinacolborane (HBpin) generates the bisboryl complex Cp*Rh(H)$_2$(Bpin)$_2$ (**2**), which reacts with neat HBpin to generate Cp*Rh(H)(Bpin)$_3$ (**3**). X-ray diffraction, density functional theory (DFT) calculations, and NMR spectroscopy suggest a weak, but measurable, B−H bonding interaction. Both **2** and **3** dissociate HBpin and coordinate PEt_3 or P(*p*-Tol)$_3$ to generate the conventional rhodium(III) species Cp*Rh(PEt_3)(H)(Bpin) (**4**) and Cp*Rh[P(*p*-tol)$_3$](Bpin)$_2$ (**5**). Compounds **2** and **3** also react with alkanes and arenes to form alkyl- and arylboronate esters at temperatures similar to or below those of the catalytic borylation of alkanes and arenes. Further, these compounds were observed directly in catalytic reactions. The enthalpies and free energies for generation of the 16-electron intermediate and for the C−H bond cleavage and B−C bond formation have been calculated with DFT. These results strongly suggest that the C−H bond cleavage process occurs by a metal-assisted σ-bond metathesis mechanism to generate a borane complex that isomerizes if necessary to place the alkyl group cis to the boryl group. This complex with cis boryl and alkyl groups then undergoes B−C bond formation by a second σ-bond metathesis to generate the final functionalized product.

Introduction

The development of selective transformations of alkanes would allow the generation of useful reagents from completely unfunctionalized materials.[1] The selective cleavage of the primary C−H bonds of alkanes by several types of systems has been reported,[2,3] but the extension of this reaction to a catalytic process has been challenging. New elementary processes that cleave with high selectivity one type of C−H bond over another and deliver a functional group to the position at which the C−H bond is cleaved would create systems capable of selective catalytic functionalization of unactivated C−H bonds.

Oxidation of alkanes by metal oxo complexes occurs with many catalysts, but these reactions tend to cleave the weaker C−H bonds of alkanes.[4] Preferential reaction at a secondary C−H bond leads to product mixtures, unless reactions are conducted with symmetric cyclic alkanes. Enzymes can cleave terminal C−H bonds as a result of shape selectivity,[5] but systems that are suitable for synthetic applications, because they lack cofactors[6] or can be expressed in *Escherichia coli*,[7] have begun to be developed only recently. Moreover, the terminal selectivity depends on the length of the alkane.[5]

We reported that rhodium complexes generated in situ from Cp*Rh(η^4-C_6Me_6), Cp*Rh(C_2H_4)$_2$, or [Cp*RhCl_2]$_2$ and either pinacolborane (HBpin) or bispinacol diborane(4) (B_2pin_2) (eq 1) catalyze the uniquely regioselective conversion of alkanes

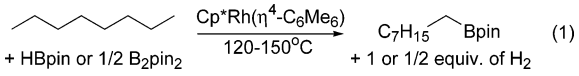

(1)

to terminal alkylboronate esters.[8] The observation of C−H activation with boryl compounds originated from studies aimed at probing the potential of the unoccupied p-orbital of a covalent ligand to create new reaction chemistry.[9,10] A boryl group is

† Yale University.
‡ Texas A&M University.

(1) (a) Arndtsen, B. A.; Bergman, R. G.; Mobley, T. A.; Peterson, T. H. *Acc. Chem. Res.* **1995**, *28*, 154. (b) Crabtree, R. H. *Chem. Rev.* **1985**, *85*, 245. (c) Shilov, A. E.; Shul'pin, G. B. *Chem. Rev.* **1997**, *97*, 2879. (c) Labinger, J. A.; Bercaw, J. E. *Nature* **2002**, *417*, 507.
(2) (a) Bergman, R. G.; Seidler, P. F.; Wenzel, T. T. *J. Am. Chem. Soc.* **1985**, *107*, 4358. (b) Wenzel, T. T.; Bergman, R. G. *J. Am. Chem. Soc.* **1986**, *108*, 4856. (c) Jones, W. D.; Hessell, E. T. *J. Am. Chem. Soc.* **1993**, *115*, 554.
(3) Bennett, J. L.; Wolczanski, P. T. *J. Am. Chem. Soc.* **1997**, *119*, 10696.
(4) (a) Gardner, K. A.; Mayer, J. M. *Science* **1995**, *269*, 1849. (b) Mayer, J. M. *Acc. Chem. Res.* **1998**, *31*, 441.
(5) Fisher, M. B.; Zheng, Y.-M.; Rettie, A. E. *Biochem. Biophys. Res. Commun.* **1998**, *248*, 352.
(6) (a) Joo, H.; Lin, Z.; Arnold, F. H. *Nature* **1999**, *399*, 670. (b) Peters, M. W.; Meinhold, P.; Glieder, A.; Arnold, F. H. *J. Am. Chem. Soc.* **2003**, *125*, 13442.
(7) Staijen, I. E.; van Beilen, J. B.; Witholt, B. *Eur. J. Biochem.* **2000**, *267*, 1957.
(8) Chen, H.; Schlecht, S.; Semple, T. C.; Hartwig, J. F. *Science* **2000**, *287*, 1995.
(9) (a) Hartwig, J. F.; Huber, S. *J. Am. Chem. Soc.* **1993**, *115*, 4908. (b) Hartwig, J. F.; Waltz, K. M.; Muhoro, C. N. In *Advances in Boron Chemistry*; Siebert, W., Ed.; The Royal Society of Chemistry: Cambridge, U.K., 1997; p 373.

10.1021/ja045090c CCC: $30.25

strongly electron donating.[11] Yet, it may also display some Lewis acidity.[12,13] Further, the coordination number of a boryl group may expand in a fashion similar to the way a transition-metal center expands its coordination number during many reactions.

We have sought to identify the rhodium complexes that are involved in the functionalization of alkanes. This information would allow concrete conclusions about the elementary steps that comprise the catalytic cycle and would reveal the origin of the unusually high reactivity of boryl complexes toward the cleavage of alkane C−H bonds. Yet, to date, isolation of potential intermediates in these reactions in pure form has not been reported.[8,14] Identification of the rhodium complexes in these catalytic reactions could lead to detailed information on the mechanism of the C−H bond cleavage and functionalization steps and the potential role of unsaturation at the boryl ligand.

We report a combination of experimental and theoretical studies on the synthesis, structures, and reactivity of two rhodium boryl complexes that are likely intermediates in the catalytic borylation of alkanes. Both compounds react with alkanes and arenes to generate alkyl- and arylboronate esters, and each complex has been observed directly by ^{1}H NMR spectroscopy during the catalytic process. These studies provide evidence for a new mechanism for C−H bond cleavage in a catalytic process and the ability of the boryl ligand to couple rapidly with an alkyl intermediate to form functionalized products.

Results and Discussion

Isolation of rhodium boryl complexes that could be intermediates in the regioselective borylation of alkanes catalyzed by Cp*Rh(η^4-C_6Me_6) (**1**) or related Cp*Rh complexes required a method to generate the boryl complexes faster than they react with solvent C−H bonds. We followed two strategies to generate these compounds. First, we heated **1**,[15,16] Cp*Rh(C_2H_4)$_2$, Cp*Rh($SiEt_3$)$_2$$H_2$,[17] Cp*Rh($C_2H_3SiMe_3$)$_2$,[18] and [Cp*Rh$Cl_2$]$_2$[19] with HBpin and with B_2pin_2 in cycloalkanes that lack primary C−H bonds at temperatures similar to or below those of the catalytic process. Second, we irradiated **1** with a mercury arc lamp at room temperature or below in the presence of pinacolborane and bispinacol diborane(4).

1. Thermal Reactions of Cp*Rh Complexes with HBpin and B_2pin_2. As summarized in eq 2, reaction of hexamethylbenzene complex **1**[15,16] with HBpin in octane at 95 °C generated two major products. We were unable to separate the two, but several spectral features that will be presented in detail below suggested that these complexes were the bisboryl complex *trans*-Cp*Rh(H)$_2$(Bpin)$_2$ (**2**) and the trisboryl complex Cp*Rh(H)(Bpin)$_3$, (**3**). Other thermal chemistry was less well defined. Reaction of **1** with an excess of B_2pin_2 generated trisboryl **3** as the predominant product, but this material was accompanied by other Cp* complexes, and **3** could not be isolated from these mixtures. Reactions of the bisethylene complex Cp*Ru(C_2H_4)$_2$ and HBpin led to detectable amounts of **2** and **3**, but we were unable to accumulate a significant quantity of these compounds before they decomposed. The Rh(III) complex [Cp*RhCl_2]$_2$ is a convenient catalyst precursor for the borylation of alkanes,[20,21] but it is poorly soluble in alkanes. Although it reacts to generate soluble species that catalyze the functionalization process, the insolubility of this material in cyclohexane prevented its direct conversion to the desired boryl compounds in high yield.

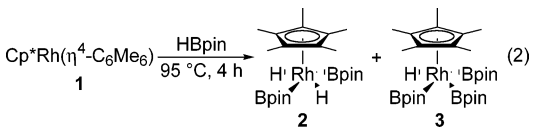

(2)

2. Photochemical Reactions of Cp*Rh Complexes with HBpin and B_2pin_2. To facilitate the dissociation of ligands from the Cp*Rh precursors at temperatures below those of the catalytic borylation of alkanes and arenes, we conducted reactions of hexamethylbenzene complex **1** with HBpin and B_2pin_2 under photochemical conditions. In contrast to heating of **1** and HBpin, irradiation of a mixture of **1** and 30 equiv of HBpin in cyclohexane with a medium-pressure mercury arc lamp generated bisboryl **2** in 95% yield by NMR spectroscopy (Scheme 1). After C_6Me_6 was removed by sublimation, bisboryl **2** was isolated by standard crystallization from pentane in 86% yield.

3. Synthesis of Trisboryl Complex 3. The thermal lability of bisboryl complex **2** was greater than that of the bissilyl compound or the olefin complexes and allowed for thermal conversion of the bisboryl **2** to the trisboryl **3**. To avoid reactions of the bisboryl **2** with alkane C−H bonds, we conducted the conversion of **2** to **3** in neat borane. The reaction of bisboryl **2** in neat HBpin for 3.5 h at 105 °C generated a 5:1 ratio of trisboryl **3** and starting **2** (Scheme 1). Evaporation of HBpin and recrystallizations from pentane generated pure trisboryl **3** in 51% yield.

Evidence for an equilibrium between the reactants HBpin and **2** and the products H_2 and **3** was obtained. Although we did not determine quantitatively the equilibrium constant between the combination of **2** and HBpin and the combination of **3** and H_2, the reaction of trisboryl **3** with hydrogen for 36 h at 40 °C in cyclohexane regenerated HBpin and the bisboryl complex in a 9:1 ratio with **3**. Further, the reactions of **2** with neat HBpin were conducted in sealed vessels, and the conversion of **2** to **3** depended on the volume of the vessel. High yields were obtained in reaction vessels with a large volume, but not those with a small volume, presumably because of the need to prevent the accumulation of a significant pressure of H_2.

4. NMR Spectral Data for Bisboryl 2 and Trisboryl 3. The bisboryl and trisboryl complexes **2** and **3** could adopt structures that reflect a rhodium(V) oxidation state with one Cp* and four conventional terminal ligands, they could adopt one of the structures in Figure 1 that are more consistent with

(10) (a) Waltz, K. M.; He, X.; Muhoro, C. N.; Hartwig, J. F. *J. Am. Chem. Soc.* **1995**, *117*, 11357. (b)Waltz, K. M.; Hartwig, J. F. *Science* **1997**, *277*, 211.
(11) Lam, K. C.; Lam, W. H.; Lin, Z. Y.; Marder, T. B.; Norman, N. C. *Inorg. Chem.* **2004**, *43*, 2541.
(12) (a) Giju, K. T.; Bickelhaupt, F. M.; Frenking, G. *Inorg. Chem.* **2000**, *39*, 4776. (b) Cundari, T. R.; Zhao, Y. *Inorg. Chim. Acta* **2003**, *345*, 70.
(13) Hartwig, J. F.; Huber, S. *J. Am. Chem. Soc.* **1994**, *116*, 3661.
(14) Kawamura, K.; Hartwig, J. F. *J. Am. Chem. Soc.* **2001**, *123*, 8422.
(15) Bowyer, W. J.; Geiger, W. E. *J. Am. Chem. Soc.* **1985**, *107*, 5657.
(16) Bowyer, W. J.; Merkert, J. W.; Geiger, W. E. *Organometallics* **1989**, *8*, 191.
(17) (a) Fernandez, M. J.; Maitlis, P. M. *J. Chem. Soc., Dalton Trans.* **1984**, 2063. (b) Fernandez, M. J.; Bailey, P. M.; Bentz, P. O.; Ricci, J. S.; Koetzle, T. F.; Maitlis, P. M. *J. Am. Chem. Soc.* **1984**, *106*, 5458.
(18) Lenges, C. P.; White, P. S.; Brookhart, M. *J. Am. Chem. Soc.* **1999**, *121*, 4385.
(19) White, C.; Yates, A.; Maitlis, P. M. *Inorg. Synth.* **1992**, *29*, 228.
(20) Shimada, S.; Batsanov, A. S.; Howard, J. A. K.; Marder, T. B. *Angew. Chem., Int. Ed.* **2001**, *40*, 2168.
(21) Kondo, Y.; Garcia-Cuadrado, D.; Hartwig, J. F.; Boaen, N. K.; Wagner, N. L.; Hillmyer, M. A. *J. Am. Chem. Soc.* **2002**, *124*, 1164.

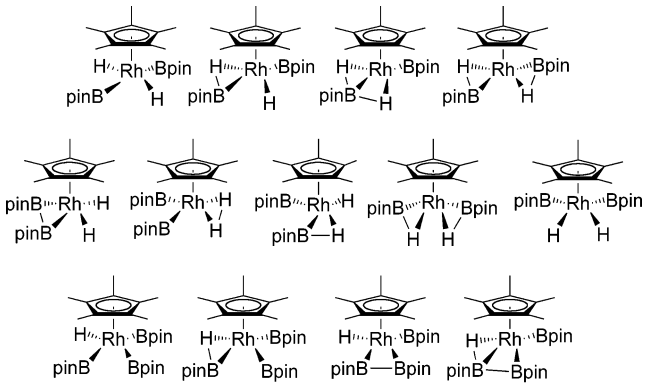

Figure 1. Various possible geometries and valence bond descriptions of bisboryl complex **2** and trisboryl complex **3**.

Scheme 1

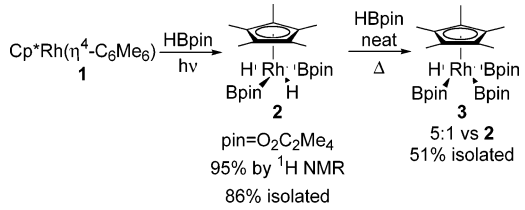

a rhodium(III) metal center, or they could adopt structures that are most consistent with a Rh(I) metal center. The rhodium(III) structures contain two terminal ligands and a borane coordinated through the B−H σ-bond, one terminal boryl group and a unit resembling a hydridoborate with partial bonding between two hydrides, two boryl ligands with partial B−B bonding, or, in the case of compound **2**, two hydrides with partial H−H bonding. The rhodium(I) structure for **2** would contain two coordinated boranes. Each of these structures should be considered because borane complexes have been characterized by X-ray diffraction and spectroscopic methods,[22−25] hydridoborate complexes are common[26] and have weak B−H bonds when the boron contains alkoxo groups,[13,27] short B−B distances have been measured by X-ray diffraction in some bisboryl complexes,[11,28] and dihydrogen complexes are now common.[29]

The X-ray diffraction data described below show that the bisboryl compound **2** adopts the trans structure as a solid. The ^{1}H NMR spectra of **2** contained a single set of pinacolmethyl groups. This spectroscopic feature is consistent with a trans structure for **2** in solution and is inconsistent with a rigid cis structure. Although it is possible that **2** undergoes fast site exchange in solution, we did not observe broadening of the pinacol methyl resonances at low temperature. Thus, the combination of NMR and X-ray diffraction data and the steric demands of the pinacolate group make a trans structure for **2** in solution most likely.

Solution NMR spectroscopic data for **2** and **3**, which contained direct scalar B−H coupling, suggested that their structures contained B−H bonding interactions. A resonance at δ 40.4 ppm was observed in the ^{11}B NMR spectrum of **2**. This resonance is consistent with a boryl group bound to the metal but does not distinguish between a transition metal boryl species or a borane complex,[30] and splitting from ^{1}H−^{11}B coupling was not resolved in the broad ^{11}B NMR signal. However, the ^{1}H NMR spectrum of complex **2** contained a doublet resonance for the hydrides at δ −11.9 ppm ($^1J_{\mathrm{Rh-H}}$ = 40.5 Hz) and a single pinacolate resonance. These data are consistent with a mutually trans arrangement of the boryl groups, and this geometry precludes a strong H−H interaction. The ^{1}H resonance for the hydride of **2** provided evidence for direct scalar ^{11}B−^{1}H coupling. The resonance for the hydride of **2** was broad, and the 40 Hz width at half-height decreased to 10 Hz upon ^{11}B decoupling. Consistent with broad lines from scalar coupling, cross-peaks were observed in the ^{1}H−^{11}B HMQC spectrum of **2**.

The ^{1}H NMR spectra of complex **3** also contained spectral features that suggested a B−H bonding interaction. The ^{1}H NMR spectrum of **3** contained a broad hydride signal at δ −11.3 that possessed a line width at half-height of 32 Hz (298 K). Like the hydride resonance of **2**, this resonance sharpened to 10 Hz upon ^{11}B decoupling.

The signals for the hydride ligands in the ^{1}H NMR spectra of many complexes with hydride and boryl groups are sharp.[20,30,31] For example, the hydride resonance in the ^{1}H NMR spectrum of the closely related compound Cp*Ir(H)$_2$(Bpin)$_2$ was sharp.[14] We have now obtained a ^{1}H−^{11}B HMQC spectrum of Cp*Ir(H)$_2$(Bpin)$_2$, and in contrast to those of **2** and **3**, this spectrum did not contain any cross-peaks. The difference between the NMR spectra of this complex and those of the rhodium analogues is consistent with a greater stability of classical structures for metals of the third row than for those of the second row.[32]

The NMR data for **3** also indicated that this complex was stereochemically nonrigid. A four-legged piano-stool geometry with one boryl group located trans to the hydride and two boryl groups trans to each other would be expected for the trisboryl complex. However, the ^{11}B NMR spectrum contained a single boryl resonance at δ 39.9 ppm, and the ^{1}H NMR spectrum contained a single set of pinacol methyl groups. Thus, the spectral data for **3** indicate that the boryl groups exchange positions within this four-legged piano stool geometry. This type

(22) Muhoro, C. N.; He, X. M.; Hartwig, J. F. *J. Am. Chem. Soc.* **1999**, *121*, 5033.
(23) (a) Muhoro, C. N.; Hartwig, J. F. *Angew. Chem., Int. Ed. Engl.* **1997**, *36*, 1510. (b) Hartwig, J. F.; He, X.; Muhoro, C. N.; Eisenstein, O.; Bosque, R.; Maseras, F. *J. Am. Chem. Soc.* **1996**, *118*, 10936.
(24) Schlecht, S.; Hartwig, J. F. *J. Am. Chem. Soc.* **2000**, *122*, 9435.
(25) Montiel-Palma, V.; Lumbierres, M.; Donnadieu, B.; Sabo-Etienne, S.; Chaudret, B. *J. Am. Chem. Soc.* **2002**, *124*, 5624.
(26) Marks, T. J.; Kolb, J. R. *Chem. Rev.* **1977**, *77*, 263.
(27) (a) Lantero, D. R.; Motry, D. H.; Ward, D. L.; Smith, M. R., III. *J. Am. Chem. Soc.* **1994**, *116*, 10811. (b) Lantero, D. R.; Ward, D. L.; Smith, M. R., III. *J. Am. Chem. Soc.* **1997**, *119*, 9699.
(28) (a) Clegg, W.; Lawlor, F. J.; Marder, T. B.; Nguyen, P.; Norman, N. C.; Orpen, A. G.; Quayle, M. J.; Rice, C. R.; Robins, E. G.; Scott, A. J.; Souza, F. E. S.; Stringer, G.; Whittell, G. R. *J. Chem. Soc.* **1998**, 301. (b) Clegg, W.; Lawlor, F. J.; Lesley, G.; Marder, T. B.; Norman, N. C.; Orpen, A. G.; Quayle, M. J.; Rice, C. R.; Scott, A. J.; Souza, F. E. S. *J. Organomet. Chem.* **1998**, *550*, 183. (c) Dai, C.; Stringer, G.; Corrigan, J. F.; Taylor, N. J.; Marder, T. B.; Norman, N. C. *J. Organomet. Chem.* **1996**, *513*, 273. (d) Lesley, G.; Nguyen, P.; Taylor, N. J.; Marder, T. B.; Scott, A. J.; Clegg, W.; Norman, N. C. *Organometallics* **1996**, *15*, 5137.
(29) (a) Heinekey, D. M.; Oldham, W. J. *Chem. Rev.* **1993**, *93*, 913. (b) Kubas, G. J. *Metal-dihydrogen and sigma-bond complexes: structure, theory, and reactivity*; Kluwer Academic: New York, 2001.
(30) Irvine, G. J.; Lesley, M. J. G.; Marder, T. B.; Norman, N. C.; Rice, C. R.; Robins, E. G.; Roper, W. R.; Whittell, G. R.; Wright, L. J. *Chem. Rev.* **1998**, *98*, 2685.
(31) The analogous iridium(III) boryl hydrides are very stable: Iverson, C. N.; Smith, M. R., III. *J. Am. Chem. Soc.* **1999**, *121*, 7696.
(32) (a) Desrosiers, P. J.; Cai, L.; Lin, Z.; Richards, R.; Halpern, J. *J. Am. Chem. Soc.* **1991**, *113*, 4173. (b) Luo, X.-L.; Crabtree, R. H. *J. Am. Chem. Soc.* **1990**, *112*, 4813.

Table 1. Structural Data for Compounds **2**−**5** by X-ray Diffraction and DFT Methods

	2	2′[a]	3	3′[a]	4	4′[a]	5	5′[a]
				Bond Distances				
Rh−B(1)	2.055(7) 2.069(6)	2.050	2.056(3) 2.059(3)	2.119	2.029(4)	2.033	2.0282(13) 2.0308(14)	2.044
Rh−B(2)	2.081(6) 2.079(6)	2.096	2.071(3) 2.065(3)	2.067			2.0282(13) 2.0332(14)	2.046
Rh−B(3)			2.059(3) 2.078(3)	2.054				
Rh−H(1)	1.41(5) 1.47(6)	1.565	1.47(3) 1.45(3)	1.619	1.42(3)	1.565		
Rh−H(2)	1.49(5) 1.59(6)	1.610						
B(1)−H(1)	1.65(4) 1.70(6)	1.896	1.69(3) 1.53(3)	1.459	2.23(3)	2.142		
B(2)−H(1)	2.20(4) 2.30(6)	2.259						
B(3)−H(1)			1.99(3) 2.06(3)	2.269				
B(1)−H(2)	2.13(5) 2.21(6)	2.331						
B(2)−H(2)	1.57(5) 1.70(6)	1.501						
Rh−P(1)					2.2306(11)	2.267	2.2414(6) 2.2359(5)	2.273
				Angles with Rh−H				
H(1)−Rh(1)−H(2)	81(3) 94(3)	95.6						
H(1)−Rh(1)−B(1)	53.1(17) 54(2)	61.6	54.3(10) 69.4(11)	43.4	78.5(12)	71.7		
H(1)−Rh(1)−B(2)	75.6(17) 79(2)	74.6	104.9(11) 100.8(11)	100.4				
H(2)−Rh(1)−B(1)	71.7(19) 73(2)	78.1						
H(2)−Rh(1)−B(2)	48.8(18) 53(2)	45.4						
H(1)−Rh(1)−B(3)			66.4(10) 47.5(11)	75.3				
				Angles with Rh−Bpin				
B(1)−Rh(1)−B(2)	105.7(2) 104.0(2)	102.6	73.63(12) 78.47(13)	76.8			76.37(5) 76.48(6)	77.5
B(1)−Rh(1)−B(3)			103.40(12) 102.27(13)	105.3				
B(3)−Rh(1)−B(2)			80.34(13) 74.79(12)	77.9				
				Angles with Rh−PR_3				
H(1)−Rh(1)−P(1)					83.7(12)	85.5		
B(1)−Rh(1)−P(1)					83.7(12)	88.1	92.82(5) 91.03(4)	88.1
B(2)−Rh(1)−P(1)							92.49(5) 92.26(4)	89.5

[a] Compounds with truncated structures calculated with DFT are named **2′**, **3′**, **4′**, and **5′**.

of stereochemical nonrigidity for compounds with such piano-stool structures is well-known.[33]

5. Structural Data for Boryl Complexes 2 and 3 from X-ray Diffraction and Theoretical Methods. a. Structure of Bisboryl 2 Determined by X-ray Diffraction. The structure of compound **2** was determined by X-ray diffraction. This complex crystallized with two independent molecules in the asymmetric unit. An ORTEP diagram of **2** is provided in Figure 2, and selected distance and angle data are provided in Table 1, along with data on other experimental and theoretical compounds described in this paper. The hydride ligands were located and refined isotropically. Compound **2** adopts the same trans, four-legged piano-stool structure in the solid state that was deduced from NMR spectroscopy. The B−Rh−B angles in the two independent molecules are 104.0(2)° and 105.7(2)°. The shorter rhodium−boron bond distances in the two structures are 2.055(7) and 2.069(6) Å, and the longer rhodium−boron distances are 2.081(6) and 2.079(6) Å. These distances are longer than the 2.047(7) Å distance of the closely related iridium complex $Cp^*Ir(H)_3(Bpin)$[14] and are longer than the 1.907−2.055 Å distances[34] of other rhodium dioxaborolanyl complexes.

Most striking, each hydride ligand is located closer to one of the boryl groups than to the other, and each boryl group is similarly located closer to one of the hydrides than to the other. The shorter B−H distances range from 1.57(5) to 1.70(6) Å, and the longer distances range from 2.13(5) to 2.30(6) Å. The two H−Rh−B angles also reflect the unsymmetrical geometry.

(33) The isoelectronic complexes $CpMoL(CO)_2R$ are known to be stereochemically nonrigid: Faller, J. W.; Anderson, A. S. *J. Am. Chem. Soc.* **1970**, *92*, 5852.

(34) CSD v5.25, November 2003.

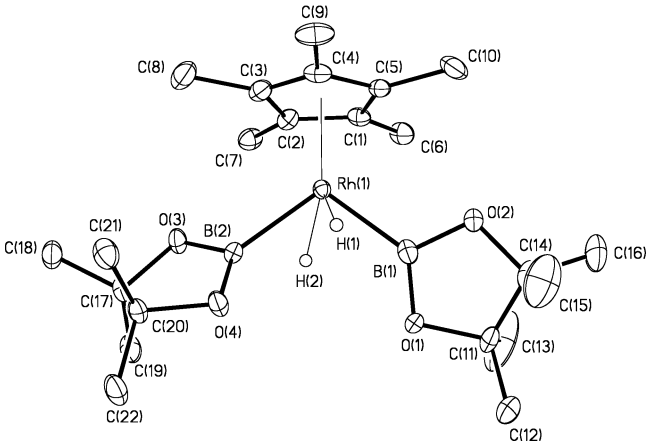

Figure 2. ORTEP drawing of one of two independent molecules of Cp*Rh-$(H)_2(Bpin)_2$ (**2**) in the asymmetric unit with 30% thermal ellipsoids.

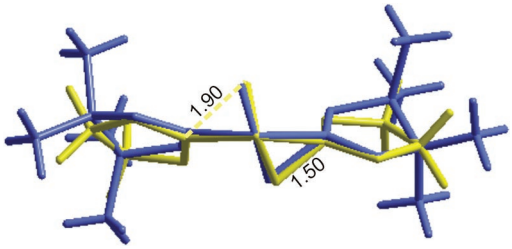

Figure 3. Overlay of experimental structure $Cp^*Rh(H)_2(Bpin)_2$ (**2**) (in blue) and calculated structure $CpRh(H)_2(B(O_2C_2H_4))_2$ (**2′**) (in yellow) with the Cp* and Cp groups removed for clarity. The calculated B−H distances are given in angstroms.

The angles that include the hydride and the nearest boron atom are between 49(2)° and 54(2)° in the two molecules, while the angles that include the hydride and the more distant cis boron atoms are between 72(2)° and 79(2)°. Thus, we conclude that the structure of complex **2** contains significant B−H bonding and that the bonding between each boryl group and one of its cis hydrides is stronger than the bonding between the boryl group and its other cis hydride.

b. Structure of 2′ Deduced by Theory. Because of the ambiguity of the metrical parameters involving hydride ligands, we conducted a computational study of the structure of this compound. Throughout this work, structures were calculated for truncated models in which Cp* was replaced by Cp and Bpin was replaced by $BO_2C_2H_4$. These compounds are labeled with a prime to distinguish them from the experimental structures; i.e., compound **2** is the experimental species $Cp^*Rh(H)_2(Bpin)_2$, and **2′** is the computed species $CpRh(H)_2(BO_2C_2H_4)_2$.

An overlay of the bottom portion of the experimental and theoretical structures of **2** and **2′** is provided in Figure 3. Clearly, the structure determined by theoretical methods corroborates the unsymmetrical orientation of the hydride ligands deduced by X-ray diffraction. As summarized in Table 1, the structure deduced from theory contained one B−H distance that is shorter than the other B−H distance. Further, one H−Rh−B angle for the hydride involved in the B−H interaction is 45.5°, while the other angle is 78.1°. The two H−Rh−B angles involving the other hydride ligand are also unsymmetrical, 61.6° and 74.6°. This trend toward an unsymmetrical positioning of the hydride between the two boryl ligands and the boryl ligands between the two hydrides in both experimental and theoretical data

Scheme 2. Exchange of the Hydrides and the Boryl Groups in $CpRh(H)_2(B(O_2C_2H_4))_2$ (**2′**) Calculated with DFT[a]

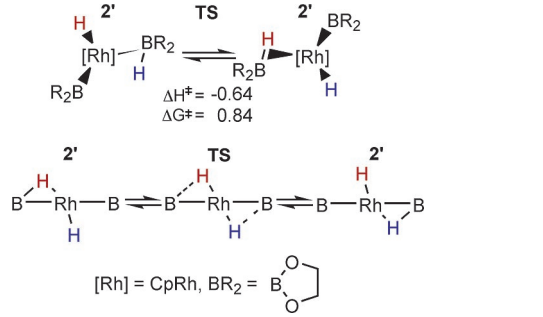

[a] Energies are in units of kcal mol^{-1}. [Rh] = CpRh, and BR_2 = $(BO_2C_2H_4)$. For clarity, the Cp ligand is not shown and is located behind the rhodium, and all other ligands are located in front of the rhodium.

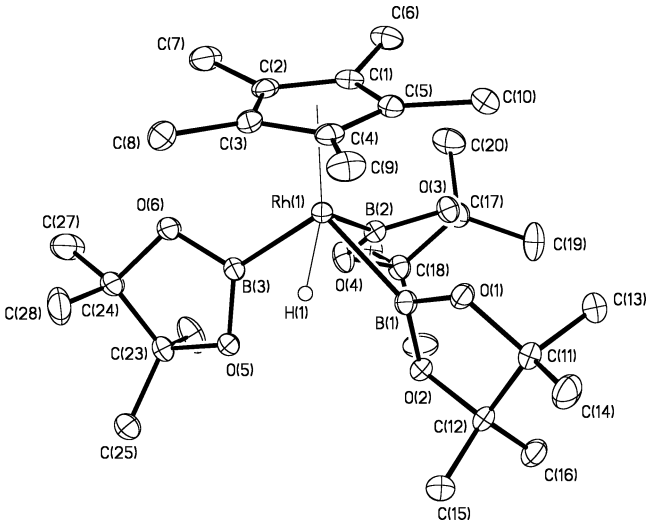

Figure 4. ORTEP drawing of one of two independent molecules of Cp*Rh-$(H)(Bpin)_3$ (**3**) in the asymmetric unit with 30% thermal ellipsoids.

supports the B−H bonding deduced from ^1H NMR spectroscopy and X-ray diffraction.

The computational work also shows that the barrier for shortening and lengthening the B−H bonds is low. As shown in Scheme 2, a concerted process by which one of the shorter B−H bond distances lengthens while the other B−H distance shortens occurs with a free energy barrier of only 0.8 kcal mol^{-1}. Therefore, the two hydrides and two boryl groups are indistinguishable in solution on the NMR time scale. It is reasonable to assume that the barrier for interconversion of the hydrogens is larger in the solid phase than it is in the gas phase because this conversion involves movement of the Bpin group, and this movement would be restricted by packing forces in the crystal.

c. Structure of Trisboryl 3 Determined by X-ray Diffraction. The structure of trisboryl complex **3** was also determined by X-ray diffraction. Like **2**, this compound crystallized with two independent molecules in the asymmetric unit. An ORTEP diagram of **3** is provided in Figure 4, and selected distance and angle data are provided in Table 1. The hydride ligand of trisboryl **3** was located and refined isotropically. Like the hydrides of **2**, the hydride in **3** appeared by X-ray diffraction to be located unsymmetrically between the two nearest boryl groups. One of the B−H distances in **3** was found to be 1.53-(3) and 1.69(3) Å in the two molecules, and the other 1.99(3)

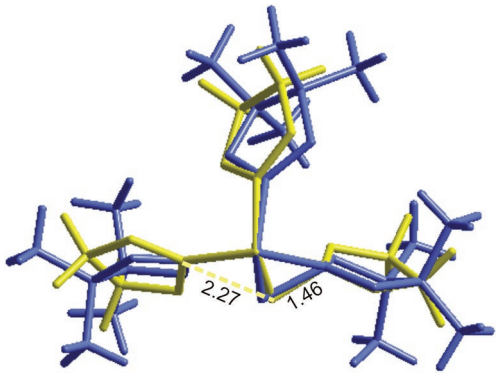

Figure 5. Overlay of experimental structure Cp*Rh(H)(Bpin)$_3$ (**3**) (in blue) and calculated structure CpRh(H)(B($O_2C_2H_4$))$_3$ (**3′**) (in yellow) with the Cp* and Cp groups removed for clarity. The calculated B−H distances are given in angstroms.

Scheme 3. Energies for the Exchange of Boryl Groups in CpRh(H)[B($O_2C_2H_4$)]$_3$ (**3′**) Calculated with DFT[a]

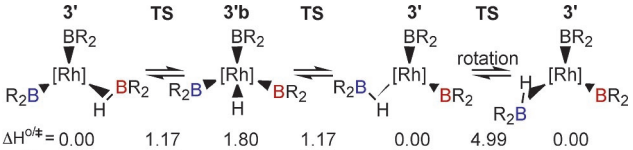

[a] Energies are in units of kcal mol^{-1}. [Rh] = CpRh, and BR_2 = ($BO_2C_2H_4$). For clarity, the Cp ligand is not shown and is located behind the rhodium, and all other ligands are located in front of the rhodium.

and 2.06(3) Å. The smaller H−Rh−B angles in the two independent molecules were found to be 47.5(8)° and 54.3(10)°, and the larger H−Rh−B angles were 66.4(10)° and 69.4(11)°. The Rh−B distances for the two boryl groups that are mutually trans are indistinguishable from the Rh−B distance of the boryl group that is trans to the hydride. Thus, the overall geometry of this species is that of a four-legged piano stool with B−H bonding of the hydride to one of its cis boryl groups that is stronger than the B−H bonding to its other cis boryl group.

d. Structure of 3′ Deduced by Theory. The structure of complex **3** was also evaluated by computational methods. An overlay of the experimental and computed structures **3** and **3′** is provided in Figure 5, and the computed distances and angles are included in Table 1. Again, the computational data support the unsymmetrical structure with partial B−H bonding indicated by X-ray diffraction. The two B−H distances deduced from theory are significantly different, 1.46 and 2.27 Å, and the two H−Rh−B angles are much different, 43.4° and 75.3°. Thus, we conclude that complex **3** tends toward a structure with two terminal boryl groups and one borane ligand.

A minimum on the energy surface was also found for a C_s symmetric, Rh(V) species, **3′b**, with equivalent and long B−H bond distances. In this C_s structure, the Rh−H bond length is 1.549 Å, the B−H distances are 2.028 Å, and the corresponding H−Rh−B angles are 66.4°. However, this species lies 1.3 kcal mol^{-1} uphill of the unsymmetrical complex **3′** (Scheme 3). The free energy barriers for interconversion of the different structures of **3** appear to be small. The free energy barrier between **3′** and **3′b** is only 2.6 kcal mol^{-1}, and the free energy barrier for rotation of the borane ligand in **3′** through a structure with the hydride close to the remote boryl group is only 4.2 kcal mol^{-1}.

Scheme 4

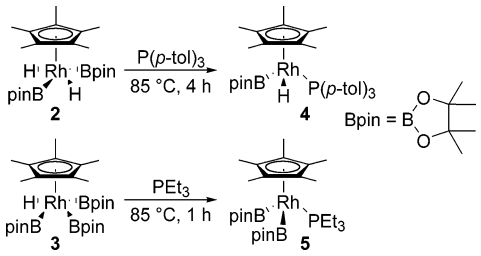

Therefore, in solution, the cis and trans boryl groups undergo rapid exchange on the NMR time scale.

The closest B−H distances in either **2** or **3** are significantly longer than the 1.24−1.31 B−H distances in manganese borane complexes (MeCp)Mn(CO)$_2$(HBR$_2$).[24] Consistent with this difference in distances, the B−H coupling in the manganese compound was stronger. A 1:1:1:1 quartet was observed for the hydride in the ^{1}H NMR spectrum of the manganese compound, and a doublet was observed for the boryl group in the ^{11}B NMR spectrum. The B−H distances in **2** and **3** are also much longer than the 1.25−1.35 Å B−H distances in two titanocene borane complexes[22,23] and the 1.35 Å distance in a ruthenium σ-borane complex.[25] However, this distance is shorter than the B−H distances of 2.013(5) and 2.004(10) Å in [(P^iPr_3)$_2$RhHCl(Bpin)] and [(P^iPr_3)$_2$RhHCl(Bcat)], which were determined by neutron diffraction and used to suggest modest H−B bonding.[35] Thus, we conclude that compounds **2** and **3** should be regarded as elongated σ-borane complexes, much like dihydrogen complexes with long H−H distances are termed "elongated" dihydrogen complexes.

6. Reactivity of Complexes 2 and 3. a. Dissociation of Borane. Boryl compounds **2** and **3** could dissociate H_2, HBpin, or B_2pin_2 by H−H, H−B, or B−B bond formation. Consistent with the apparent partial B−H bonding in the ground-state structures, complexes **2** and **3** underwent dissociation of HBpin faster than they underwent dissociation of H_2 or B_2pin_2, as summarized in Scheme 4.

Reaction of bisboryl **2** with P(*p*-tol)$_3$ for 4 h at 85 °C formed Cp*Rh[P(*p*-tol)$_3$](H)(Bpin) (**4**) in 68% yield by NMR spectroscopy and 51% isolated yield. A second rhodium species, whose NMR spectra are consistent with the formulation Cp*Rh(Bpin)$_2$[P(*p*-tol)$_3$], was formed in 17% yield. This minor compound would form by elimination of H_2 from **2**. Reaction of this complex **2** with PEt$_3$, instead of P(*p*-tol)$_3$, occurred similarly, but the boryl hydride complex generated from reaction of **2** with this trialkylphosphine was less crystalline. Assuming the elimination of hydrogen would be irreversible, these product ratios imply that the overall rate of the extrusion of HBpin from **2** is at least 4 times greater than the rate of extrusion of H_2. However, the elimination of H_2 from **2** would clearly require a rearrangement of the ground-state structure of **2** to place the hydrides cis to each other. Thus, the product ratios do not reflect the relative rate constants for the elementary steps of B−H vs H−H bond formation. Instead, they reflect the relative rate constants for elimination of HBpin vs the combination of rearrangement and elimination of H_2.

The rate of reaction of **2** in the presence of P(*p*-tol)$_3$ was faster than the rate of decomposition of **2** at this temperature in

(35) Lam, W. H.; Shimada, S.; Batsanov, A. S.; Lin, Z. Y.; Marder, T. B.; Cowan, J. A.; Howard, J. A. K.; Mason, S. A.; McIntyre, G. J. *Organometallics* **2003**, *22*, 4557.

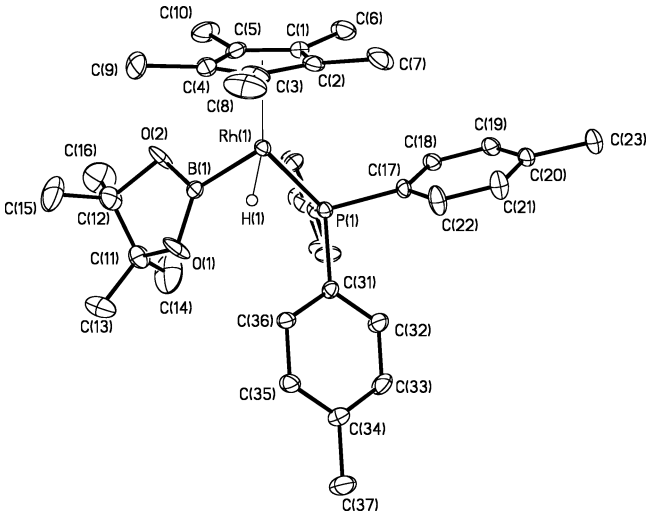

Figure 6. ORTEP drawing of Cp*Rh[P(*p*-Tol)$_3$](H)(Bpin) (**4**) with 30% ellipsoids.

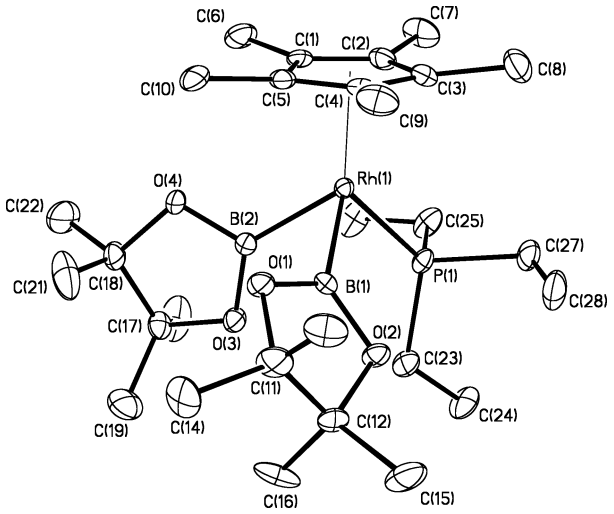

Figure 7. ORTEP drawing of Cp*Rh(PEt$_3$)(Bpin)$_2$ (**5**) with 30% ellipsoids.

Scheme 5

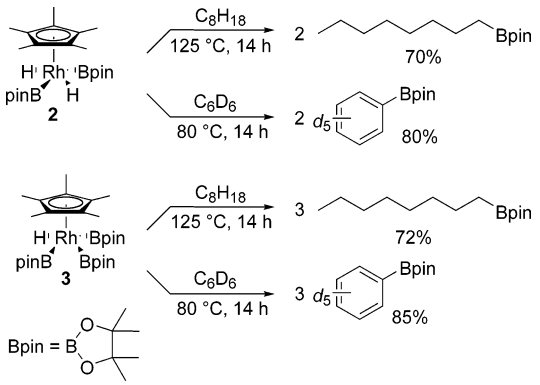

cyclohexane in the absence of added phosphine. After heating of **2** with P(*p*-tol)$_3$ for 24 h at 45 °C, only 5% of the bisboryl complex remained, but after heating of bisboryl **2** without phosphine for the same time and temperature, 60−70% remained. Complex **2** is an 18-electron species, and previous replacements of boranes in 18-electron complexes with phosphine have occurred by dissociative paths.[22,24] Considering this information, the faster reaction of **2** in the presence of added ligand than in the absence of added ligand implies that dissociation of HBpin from **2** occurs reversibly when it is heated alone in cyclohexane.

Trisboryl complex **3** also underwent dissociation of HBpin. Heating of trisboryl **3** at 85 °C with 1 equiv of PEt$_3$ for 1 h formed Cp*Rh(Bpin)$_2$(PEt$_3$) (**5**) in 77% isolated yield. (Reaction with P(*p*-tol)$_3$ occurred in a similar fashion, but the substitution product was isolated in only 51−54% yield, and the isolated material was not analytically pure.) Thus, dissociation of HBpin from trisboryl **3** is much faster than dissociation of B_2pin_2, even though this complex could undergo dissociation of the diborane(4) species without the need for isomerization. One could envision that the combination of dissociation of the diborane(4) species and coordination of PEt$_3$ is not observed because it is thermodynamically unfavorable. However, such a proposal would be inconsistent with a large thermodynamic driving force calculated with DFT for the elimination of $B_2(OR)_4$ and subsequent coordination of phosphine (vide infra).

Dissociation of borane from **3** was consistently faster than dissociation of borane from **2**. The approximate half-life for decay of **3** at 55 °C was 40 min, while the approximate half-life for decay of **2** at 55 °C was 127 min, as determined by monitoring the reactions periodically by ^{1}H NMR spectroscopy with added PEt$_3$ and dodecahydrotriphenylene as internal standard. These rates are in agreement with the calculated energies for dissociation (vide infra).

b. Structures of the Ligand Substitution Products. The structures of the rhodium(III) boryl complexes **4** and **5** resulting from ligand substitution were determined. An ORTEP diagram of compound **4** is provided in Figure 6, and metrical parameters are included in Table 1. Compound **4** possesses a three-legged piano-stool geometry. Consistent with a sharp ^{1}H NMR resonance for the hydride in **4**, the structure of compound **4** is more classical than those of **2** and **3**. The B−H distance in compound **4** is much longer (X-ray = 2.23(3) Å; computed for **4′**, 2.14 Å) than the shorter of the B−H distances in compound **2**, and the Rh−B distance is measurably shorter. Thus, the X-ray diffraction data and DFT calculations imply that compound **4** contains terminal hydride and boryl ligands without any residual B−H bonding. This difference in the bonding of **2** and **4** implies a lower formal oxidation state of **4** and would result from a lower coordination number of **4** and strong electron donation from a phosphine ligand.

An ORTEP diagram of **5** is shown in Figure 7, and metrical parameters are included in Table 1. This complex crystallized with two independent molecules in the asymmetric unit. Some complexes with two cis boryl groups contain a B−B interaction,[11,28] but the structure of **5** contains a long B−B distance and no evidence for such partial B−B bonding. The Rh−B distances in **5** are similar to that in **4** and are shorter than the Rh−B distances in **2** and **3**. The shorter M−B distances in compound **5**, relative to those in **2** and **3**, are likely to stem from the presence of two simple terminal boryl groups in a conventional rhodium(III) species. This structure would again be favored by the lower coordination number in **5** than in **3** and by the strong electron donation from the phosphine ligand.

c. Reactions of 2 and 3 with Hydrocarbons. The reactions of boryl complexes **2** and **3** with hydrocarbons are summarized in Scheme 5. Both complexes reacted with linear alkanes and with benzene to form octyl- and phenylboronate esters, respectively. Reactions with alkanes were slower than reactions with

Scheme 6

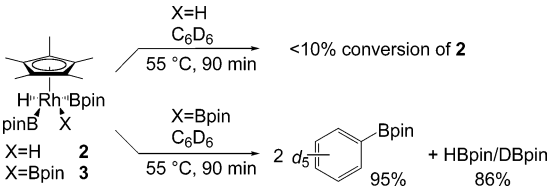

arenes, and the reactions of bisboryl complex **2** were slower than those of trisboryl **3**. The relative rates for reaction of **2** and **3** with hydrocarbons parallel the relative rates for dissociation of borane from **2** and **3**.

Heating of **2** at 125 °C in octane for 14 h formed 2 equiv of octylboronate ester in 70% yield, as determined by GC (Scheme 5). The product boronate ester has been generated previously by catalytic studies[8] and by independent synthesis. Heating of **2** at 80 °C in C_6D_6 for 14 h produced 2 equiv of PhBpin-d_5 in 80% yield. By stoichiometry, the rhodium product from these reactions would be Cp*RhH_4. However, this complex has never been prepared and is presumably unstable because a variety of bridging hydrides are formed upon reduction of Cp*RhX_2 compounds.[36] Thus, a series of rhodium complexes are generated from the stoichiometric reactions of **2** with hydrocarbons, and we have not been able to characterize them. In a catalytic system, the product rhodium fragment would likely be trapped with the borane reagent to regenerate **2** or **3**.

Reaction of trisboryl complex **3** with octane at 125 °C for 14 h formed 3 equiv of octylboronate ester in 72% yield, as determined by GC methods. Reaction of **3** with C_6D_6 at 80 °C for 14 h produced 3 equiv of PhBpin-d_5 in 85% yield. The rhodium hydride product from reaction of **3** was also unstable, and several signals for Cp*−rhodium complexes were observed at the end of the reactions of **3** with octane and C_6D_6. At 125 °C, we were unable to observe any accumulation of bisboryl **2** from reaction of **3** with octane. However, at 90 °C 35−40% of bisboryl complex **2** was observed. Along with **2**, octylBpin was generated in a 1.26:1 ratio to the amount of starting trisboryl **3**. After 3 h, however, the solution contained only 10% of the bisboryl complex because this complex also reacts with octane.

We conducted reactions of boryl complexes **2** and **3** with hydrocarbons at lower temperatures to distinguish their relative reactivities. These experiments, summarized in Scheme 6, revealed that trisboryl **3** reacted faster than bisboryl **2**. After 90 min at 55 °C, trisboryl **3** underwent complete reaction in C_6D_6 to form 2 equiv of PhBpin-d_5 in greater than 95% yield. This reaction also generated 1 equiv of a mixture of HBpin and DBpin in a roughly 1:1 ratio in 86% yield, as determined by ^{1}H and ^{11}B NMR spectroscopy. The 2 equiv of PhBpin-d_5 and 1 equiv of the combination of HBpin and DBpin account for all three boryl groups of the starting complex **3**. Under the same reaction conditions, more than 90% of bisboryl **2** remained.

The stoichiometry of the reactions of the trisboryl complex with alkanes was less well defined. However, less than 5% of the trisboryl **3** remained after heating for 60 min at 90 °C in octane, while 35−40% bisboryl **2** remained after heating in octane under identical conditions. Thus, the reaction of the trisboryl **3** with octane is also faster than the reaction of the bisboryl **2** with octane.

(36) (a) White, C.; Gill, D. S.; Kang, J. W.; Lee, H. B.; Maitlis, P. M. *J. Chem. Soc., Chem. Commun.* **1971**, 734. (b) Gill, D. S.; Maitlis, P. M. *J. Organomet. Chem.* **1975**, *87*, 359. (c) White, C.; Oliver, A. J.; Maitlis, P. M. *J. Chem. Soc., Dalton Trans.* **1973**, 1901. (d) Churchill, M. R.; Ni, S. W. *J. Am. Chem. Soc.* **1973**, *95*, 2150.

Scheme 7

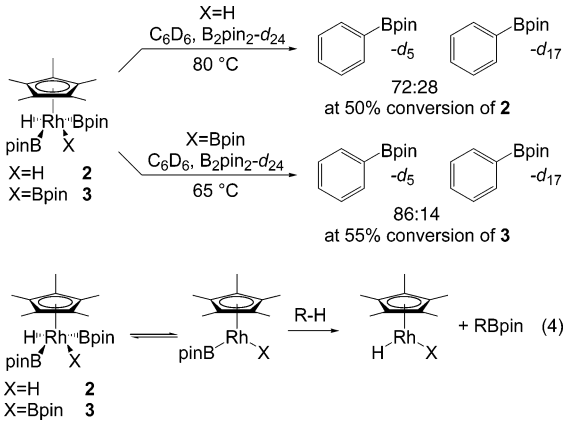

d. Mechanism of the Reactions of 2 and 3 with Hydrocarbons. One could envision that heating of **2** and **3** would generate small concentrations of free B_2pin_2 and a rhodium complex that could catalyze the reaction of alkane with the released B_2pin_2 by a pathway that does not involve **2** or **3** directly. To test this possibility, complexes **2** and **3** were heated in C_6D_6 in the presence of added B_2pin_2-d_{24}. If boryl complexes **2** and **3** react with alkanes directly, then the initial alkylboronate ester product would lack the deuterium label, but if the alkyl- and arylboronate ester products form by a catalytic reaction with the extruded diborane(4), then the initial product would possess the deuterium label.

The results of this labeling study are summarized in Scheme 7. The reaction of **2** with C_6D_6 in the presence of 1.1 equiv of B_2pin_2-d_{24} formed PhBpin-d_5 and PhBpin-d_{17} in a ratio of 72:28 after 50% conversion of **2**. Only 14% of B_2pin_2-d_{24} was consumed under these conditions in which a low 36 mM concentration of B_2pin_2-d_{24} was present. The reaction of **3** with C_6D_6 in the presence of 1.1 equiv of B_2pin_2-d_{24} formed PhBpin-d_5 and PhBpin-d_{17} in an 86:14 ratio after 55% conversion of **3**. Again only 17% of the B_2pin_2-d_{24} was consumed. Similarly, reactions of **2** and **3** with octane with 1 equiv of added B_2pin_2-d_{24} produced octylBpin and octylBpin-d_{12} in ratios near 85:15 after 55% conversion of **2** and 80% conversion of **3**.

Although one might expect that larger amounts of labeled arylboronate and alkylboronate esters would be observed due to a catalytic conversion of B_2pin_2-d_{24} to PhBpin-d_{17}, a large ratio of unlabeled to labeled arylboronate and alkylboronate ester is observed because the reaction of the rhodium product with B_2pin_2-d_{24} to regenerate the starting boryl complexes is not efficient at the low concentration of diborane(4) reagent. Most of the B_2pin_2-d_{24} is unreacted. This set of labeling experiments shows definitively that the arylboronate ester and alkylboronate ester generated from thermolysis of **2** and **3** in benzene and octane is generated from an intact boryl complex generated from **2** and **3**. The combination of this result and our studies on the dissociation of HBpin from these complexes (vide supra) implies that the intermediate boryl complex that reacts with the alkane or arene is the 16-electron species generated by dissociation of HBpin from **2** and **3**.

Because the reactions of **2** and **3** with alkanes are slower than those with arenes, the rate-determining step of the reactions of alkanes must involve the hydrocarbon and cannot be dissociation

of borane. In this case, the reaction of the 16-electron intermediate with an alkane would be preceded by reversible dissociation of borane. This assertion is consistent with the conclusion that dissociation of borane from **2** occurs reversibly upon heating in cyclohexane (vide supra). Moreover, this assertion predicts that added HBpin would inhibit the reactions of these complexes with alkanes.

To test this proposal, we conducted reactions of the trisboryl complex **3** with octane in the presence of added HBpin and compared the qualitative rates in the presence and absence of added HBpin. We did not conduct quantitative kinetic studies on these reactions because a series of rhodium products are formed. Further, the conditions of reactions in the presence of added HBpin are those of a catalytic borylation of an alkane or arene with HBpin as reagent, not a simple stoichiometric process. Because the reaction conditions are those of the catalytic borylation by HBpin, a difference in rates for the decay of **3** in the presence and absence of added HBpin could result from regeneration of **3** in the presence of HBpin, instead of consumption of **3** by reaction of all three boryl groups, as occurs in the absence of added borane. However, the catalytic reactions with HBpin are much slower than those with B_2pin_2 and require high temperatures. Therefore, it is likely that a slower reaction of **3** with added HBpin would be due to an effect of the added HBpin on the preequilibrium and not on regeneration of the trisboryl.

The reaction of **3** with octane was slower when conducted with added HBpin than when conducted without added HBpin. In one representative experiment, heating of a 13 mM solution of trisboryl **3** in octane at 100 °C for 1 h without added HBpin led to the generation of HBpin and a 15.7 mM solution of octylBpin. This quantity of octylBpin corresponds to a 60% yield for a reaction that generates 1 equiv of HBpin and converts the remaining two boryl groups to octylBpin. In contrast, reaction of an identical solution of **3** with 10 equiv (130 mM) of HBpin for the same time and temperature led to only a 5.6 mM concentration of octylBpin. Therefore, our data are consistent with a pathway involving reversible dissociation of borane and subsequent reaction of the resulting 16-electron boryl intermediate with alkane or arene, but conclusions from these experiments must be drawn tentatively.

The relationship between the inhibition of the reactions of **3** with hydrocarbons by HBpin and the mechanism of the catalytic borylation of alkanes in the presence of Cp*Rh(η^4-C_6Me_6) is significant. The stoichiometry of reactions of B_2pin_2 with alkanes to form R−Bpin leads to the formation of HBpin as a byproduct. The mechanistic data presented here suggest that the HBpin generated as byproduct may inhibit the borylation of alkanes. Moreover, these data imply that reactions of alkanes initiated with HBpin as reagent could be slower than those initiated with B_2pin_2 because the system contains a high concentration of HBpin at the beginning of the reaction.

Indeed, we have obtained data in previous work and in the current work that are consistent with these conclusions. First, the reactions of HBpin with alkanes occurred more slowly and in lower yields than reactions of B_2pin_2.[8] Second, reactions of octane with B_2pin_2 catalyzed by **2** and **3** were slower when conducted with added HBpin. For example, the reaction of octane with B_2pin_2 for 90 min at 105 °C in the presence of 30 mol % **2** led to 73% conversion of the diboron compound in the absence of HBpin, but to 31% conversion in the presence of 11 equiv of HBpin. The reaction of B_2pin_2 with octane at 90 °C for 90 min in the presence of 30 mol % trisboryl **3** led to roughly 50% conversion of the diboron compound in the absence of added HBpin but to only 20% conversion in the presence of 11 equiv of added HBpin.

The effect of HBpin on the reactions of arenes is less straightforward. The reaction of trisboryl **3** with benzene occurs at roughly the same rate as the reaction of **3** with phosphines. These similar rates imply that dissociation of borane may be rate limiting, and consistent with this assertion, the reaction of **3** with C_6D_6 appeared to occur at the same rate with or without added HBpin. If so, then the accumulation of HBpin would not affect the catalytic reactions of arenes, and the reactions of arenes with HBpin would occur at the same rate as the reactions of arenes with B_2pin_2. The similarities and differences between the reactions of arenes with B_2pin_2 and HBpin catalyzed by Cp*Rh complexes and detailed kinetic studies on the reactions of **3** with added HBpin will be the subject of future studies.

An inverse kinetic order in a reactant is unusual. In this case, the reaction order results from the need to dissociate HBpin from the metal prior to the rate-limiting step. A similar effect of added HBpin was observed during a titanium-catalyzed hydroboration that involved borane complexes as intermediates and dissociation of borane prior to reaction with olefin or alkyne.[37] In other contexts, this kinetic behavior has been observed during studies of carbonylations and hydroaminations. Under some conditions carbonylation reactions are inhibited by CO, even though it is a reagent, because CO is a ligand that must dissociate to allow coordination and insertion of olefin.[38] An inverse order in amine was observed under some conditions during zirconocene-catalyzed hydroamination of alkynes because free amine and the reactive zirconocene arylimido intermediate are generated reversibly from a bisarylamido complex prior to the turnover-limiting reaction of the imido complex with alkyne.[39]

7. Direct Observation of 2 and 3 in Catalytic Reactions. In addition to demonstrating that the boryl compounds **2** and **3** react with alkanes and arenes to form products that are analogous to those formed from the catalytic cycle, we have shown that these species are present in catalytic reactions. Reactions initiated with hexamethylbenzene precatalyst **1** or boryl complexes **2** and **3** in pentane were run to partial conversion, and ^{1}H NMR spectra were obtained on the reaction solutions. The amounts of complexes **2** and **3** were approximated by the intensity of the Cp* signals of **2** and **3**, relative to the signal of dodecahydrotriphenylene internal standard, in ^{1}H NMR spectra obtained after evaporation of pentane and dissolution of the residue in C_6D_6. In addition, the conversion of B_2pin_2 to pentylBpin was determined by GC analysis of an aliquot of the pentane solution.

Reactions initiated with precatalyst **1** were run at 125 °C to 40% conversion of B_2pin_2. After this time, complexes **2** and **3** were observed, but the sum of the intensities of the ^{1}H NMR signals of these two complexes accounted for only 10% of the starting rhodium. The same reaction was conducted at 105 °C with isolated **2** as catalyst and was analyzed in a similar fashion.

(37) Hartwig, J. F.; Muhoro, C. N. *Organometallics* **2000**, *19*, 30.
(38) Ikatchenko, I. In *Comprehensive Organometallic Chemistry*; Wilkinson, G., Stone, F. G. A., Abel, E., Eds.; Pergamon: New York, 1982; Vol. 8, p 140.
(39) Walsh, P. J.; Baranger, A. M.; Bergman, R. G. *J. Am. Chem. Soc.* **1992**, *114*, 1708.

Scheme 8. Energetics for Generation of the 16-Electron Intermediate Deduced by DFT[a]

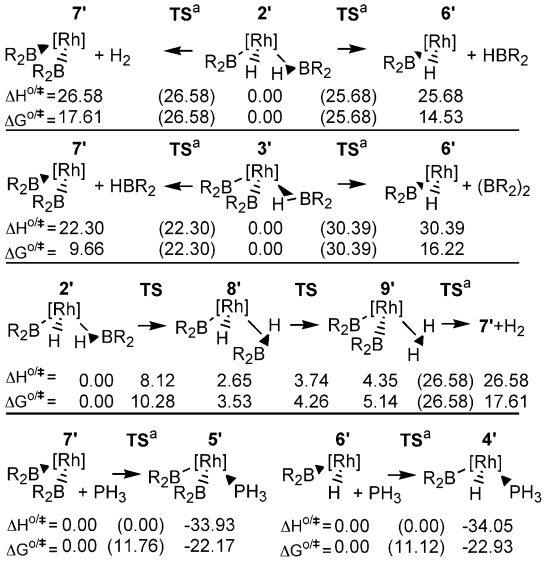

[a] Energies are in units of kcal mol^{-1} ([Rh] = CpRh, BR_2 = $(BO_2C_2H_4)$). A superscript Roman "a" following "TS" indicates that the energies are determined using the method described in the Computational Details and in Figure 10.

In this case, the sum of the resonances of **2** and **3** accounted for about 40% of the starting rhodium after 40% conversion of B_2pin_2. Finally, the same reaction was conducted at 90 °C with complex **3** as catalyst. In this case, the sum of the resonances of **2** and **3** accounted for 80% of the starting rhodium.

Although the observation of a complex in a catalytic system does not alone imply that it is an intermediate in the catalytic cycle, several pieces of data do imply that these species are intimately connected with the catalytic cycle. First, the system that leads to reaction at the lowest temperature—the reaction catalyzed by **3**—contains the largest amount of the two boryl complexes. Second, both complexes **2** and **3** are chemically and kinetically competent to be intermediates in reactions conducted with C_6Me_6 complex **1** as precatalyst. Third, the most reactive catalyst was also the complex that reacted with hydrocarbons at the lowest temperatures during studies of the stoichiometric chemistry. The lower rate of the reaction catalyzed by **1** indicates that the rate and yield of the conversion of precatalyst **1** to the active catalyst limit the concentration of the active catalyst, limit the turnover numbers for reactions initiated with **1**, and influence the reaction rate.

8. Theoretical Studies of the Reactivity of 2′ and 3′. Several mechanistic issues that were unresolved by the experimental data were addressed by computational studies. DFT calculations[40] were conducted on the dissociation of H_2, borane, and diborane from **2′** and **3′**, on the C−H bond cleavage by the resulting 16-electron intermediates, and on the B−C bond-forming step.

The results from calculations of the reactions of slightly truncated models of the bis- and trisboryl complexes with methane are summarized in Schemes 8 and 9. Scheme 8 shows the reactions that generate the 16-electron intermediates, and Scheme 9 shows the relative energies of the species involved in the reactions of the 16-electron intermediates. In the computed structures, Cp* was replaced by Cp, and the pinacolboryl group was replaced by an unsubstituted dioxaborolanyl unit.

a. Calculations on the Dissociation of H_2, HBpin, and B_2pin_2. The experimental data presented in preceding sections and computational data presented in this section of this paper are consistent with generation of a 16-electron reactive intermediate from **2** and **3** by dissociation of borane. The free energy of dissociation of borane from bisboryl **2′** to give the 16-electron boryl hydride complex **6′** is computed to be lower than the free energy of dissociation of dihydrogen. The calculated difference in the activation free energy of these two dissociation paths at standard states is small ($\Delta G^{\ddagger}$ from **2′** to $\mathbf{TS}_{2'-7'}$ − $\Delta G^{\ddagger}$ from **2′** to $\mathbf{TS}_{2'-6'}$ = 26.68 − 25.58 = 0.9 kcal mol^{-1}). This value is relatively independent of temperature, and the calculated $\Delta(\Delta G^{\ddagger})$ at 85 °C of 1.3 kcal mol^{-1} is remarkably close to the 0.9 kcal mol^{-1} value that would give rise to the experimentally observed 4:1 ratio of products from replacement of borane and dihydrogen by phosphine.

The barrier for dissociation of borane from trisboryl **3′** to give unsaturated bisboryl intermediate **7′** was smaller than that for dissociation of borane from the bisboryl **2′** to give monoboryl intermediate **6′**. The difference in barriers (∼3 kcal mol^{-1}) is larger than that which would give rise to the roughly 5−10-fold greater rate constant for the reaction of the trisboryl **3** than for reaction of the bisboryl **2**, but the calculated trend in this study matches that from the experiment. Significant for understanding the chemistry of the trisboryl complex, the barrier for elimination of B_2pin_2 to generate the boryl hydride intermediate **6′** is roughly 8 kcal mol^{-1} higher than the barrier for elimination of borane. For this reason, no phosphine-ligated boryl hydride complex **4** was obtained when trisboryl complex **3** was heated in the presence of added phosphine. Furthermore, the origin of the lack of formation of **4** from this reaction is kinetic and not thermodynamic. The enthalpy (ΔH) for coordination of phosphine to **6′** is 34 kcal mol^{-1}, and this large exothermicity would make the dissociation of B_2pin_2 and coordination of phosphine to the resulting intermediate overall exoergic.

b. Calculation of the Mechanism of the C−H Bond Cleavage and B−C Bond Formation. Our experimental data provided no information on the intimate mechanism of the C−H bond cleavage pathway. Thus, we conducted theoretical studies to provide information on the pathway by which the 16-electron intermediates react with a model alkane, methane.[41] Several calculations of the pathways of C−H activation by metal boryl compounds have now been reported by other researchers.[42−44] In addition, we have reported computational studies[45] on the formation of a methylboronate ester from methane and CpM-

(40) Frisch, M. J.; Trucks, G. W.; Schlegel, H. B.; Scuseria, G. E.; Robb, M. A.; Cheeseman, J. R.; Zakrzewski, V. G.; Montgomery, J. A., Jr.; Stratmann, R. E.; Burant, J. C.; Dapprich, S.; Millam, J. M.; Daniels, A. D.; Kudin, K. N.; Strain, M. C.; Farkas, O.; Tomasi, J.; Barone, V.; Cossi, M.; Cammi, R.; Mennucci, B.; Pomelli, C.; Adamo, C.; Clifford, S.; Ochterski, J.; Petersson, G. A.; Ayala, P. Y.; Cui, Q.; Morokuma, K.; Malick, D. K.; Rabuck, A. D.; Raghavachari, K.; Foresman, J. B.; Cioslowski, J.; Ortiz, J. V.; Stefanov, B. B.; Liu, G.; Liashenko, A.; Piskorz, P.; Komaromi, I.; Gomperts, R.; Martin, R. L.; Fox, D. J.; Keith, T.; Al-Laham, M. A.; Peng, C. Y.; Nanayakkara, A.; Gonzalez, C.; Challacombe, M.; Gill, P. M. W.; Johnson, B. G.; Chen, W.; Wong, M. W.; Andres, J. L.; Head-Gordon, M.; Replogle, E. S.; Pople, J. A. *Gaussian 98*, revisions A.7 and A.11.3; Gaussian, Inc.: Pittsburgh, PA, 1998.
(41) The barrier for primary C−H bond activation of propane ($\Delta H^{\ddagger}$ = 11.9 kcal mol^{-1}) is very similar to the barrier for C−H bond activation of methane ($\Delta H^{\ddagger}$ = 11.1 kcal mol^{-1}).
(42) Tamura, H.; Yamazaki, H.; Sato, H.; Sakaki, S. *J. Am. Chem. Soc.* **2003**, *125*, 16114.
(43) (a) Lam, W. H.; Lin, Z. Y. *Organometallics* **2003**, *22*, 473. (b) Lam, W. H.; Lam, K. C.; Lin, Z.; Shimada, S.; Perutz, R. N.; Marder, T. B. *Dalton Trans.* **2004**, 1556.
(44) Wan, X.; Wang, X.; Luo, Y.; Takami, S.; Kubo, M.; Miyamoto, A. *Organometallics* **2002**, *21*, 3703.

Scheme 9. Mechanism for the C−H Bond Cleavage and B−C Bond Formation Steps Deduced by DFT[a]

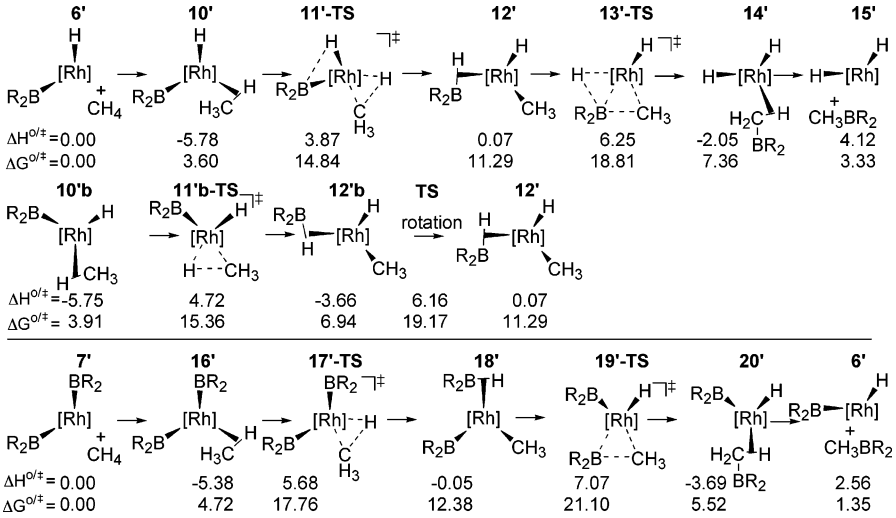

[a] Energies are in units of kcal mol^{-1}. [Rh] = CpRh, and BR_2 = ($BO_2C_2H_4$). For clarity, the Cp ligand is not shown and is located behind the rhodium, and all other ligands are located in front of the rhodium.

$(CO)_nB(O_2R)$ (M = Fe, n = 2; M = W, n = 3; R = $-CH_2-CH_2-$). The barriers for a pathway involving a metal-assisted σ-bond metathesis were lower than barriers for pathways involving a sequence of oxidative addition and reductive elimination calculated by others.[43a]

Results on the steps of C−H cleavage and B−C bond formation for the current system are summarized in Scheme 9. Again, the theoretical data favor reaction of methane with the 16-electron intermediates **6′** and **7′** by pathways related to those in a previous study[45] that involve the unoccupied p-orbital on boron. The structures of **10′** to **14′** that are computed to be intermediates and transition states in this process are shown in Figure 8. After coordination of methane to either the monoboryl hydride intermediate **6′** or the bisboryl intermediate **7′** to generate structures **10′** and **16′** in Scheme 9, a single transition state with no intermediates leads to the methyl hydride and methyl boryl complexes **12′** and **18′**, both of which contain a coordinated borane. Two conformational isomers, **12′** and **12′b**, can form from C−H bond cleavage of methane by **6′**. Isomer **12′** contains mutually cis methyl and boryl groups, and isomer **12′b** contains mutually trans methyl and boryl groups. Isomer **12′b** is more stable than isomer **12′** by more than 3 kcal mol^{-1}. However, a low-energy transition state for rotation of the borane ligand (6 kcal mol^{-1} higher in energy than **12′**) connects these two isomers.

After C−H bond cleavage and rotation of the borane ligand, if necessary, intermediates **12′** and **18′** undergo B−C bond formation through multicentered transition states **13′-TS** and **19′-TS** to generate complexes **14′** and **20′**. These complexes contain the product coordinated through a C−H bond of the B-methyl group. Dissociation of product is then uphill, but reaction of the 16-electron fragment resulting from dissociation of product with borane or diboron reagent would return the system to the stable 18-electron rhodium complexes **2′** and **3′**.

Following dissociation of borane to form the active species **6′** and **7′**, the individual C−H activation steps have the highest enthalpic barriers, roughly 8 kcal mol^{-1} for reaction of coordinated methane in the boryl hydride intermediate **10′** (generated initially from **2′**) and 10 kcal mol^{-1} for reaction of the coordinated methane in the bisboryl intermediate **16′** (generated initially from **3′**). Although the difference in barriers is small, these data suggest that the barrier for the elementary C−H bond cleavage step by the more reactive starting complex, trisboryl complex **3**, is higher than that for the elementary C−H

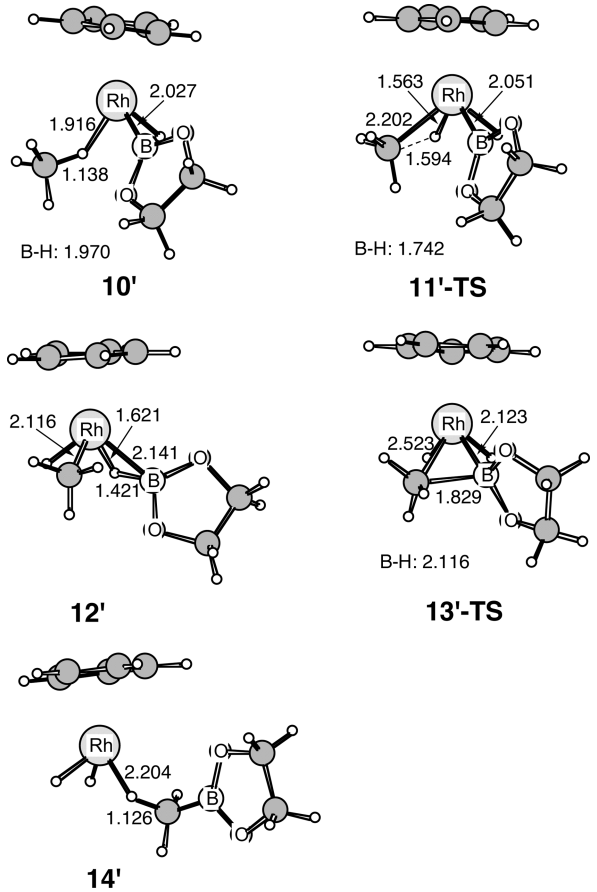

Figure 8. Structures of the intermediates and transition states in the reaction between **6′** and CH_4. Distances are in angstroms. The unlabeled gray and small white circles are carbons and hydrogens, respectively. B−H distances listed for **10′**, **11′-TS**, and **13′-TS** are for those between the boron and the Rh-bound hydrogen, which is hidden behind B in the figure.

(45) Webster, C. E.; Fan, Y.; Hall, M. B.; Kunz, D.; Hartwig, J. F. *J. Am. Chem. Soc.* **2003**, *125*, 858.

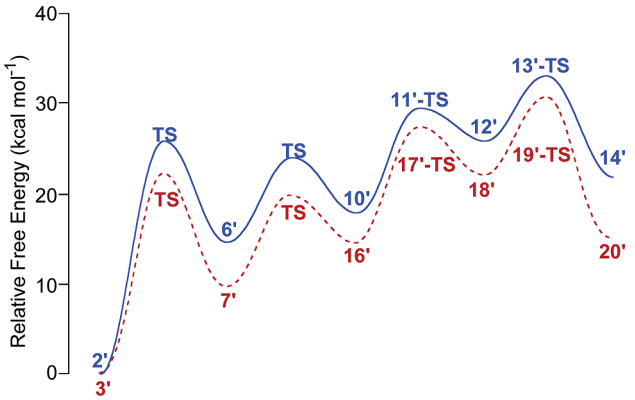

Figure 9. Relative free energies (ΔG) for the reaction of **2′** (blue solid curve) and **3′** (red dashed curve) with CH_4. For clarity, dissociated molecules and methane are omitted.

bond cleavage step by the less reactive starting complex, bisboryl **2**. If so, then the more favorable dissociation of borane from the trisboryl complex **3** would lead to the higher overall reactivity of **3** with alkanes (Figure 9), not a lower barrier for cleavage of the C−H bond.

The transition state with the highest free energy on the functionalization pathway is the transition state for B−C bond formation (**13′-TS** and **19′-TS** in Figure 9). Again, the barriers for the individual B−C bond formation steps are calculated to be higher for the more stable intermediate **7′** generated from the trisboryl **3′**. The barrier from **12′** to **13′-TS** for reaction of the intermediate generated from the bisboryl **2′** is 2.6 kcal mol^{-1} lower than that from **18′** to **19′-TS** for reaction of the intermediate generated from the trisboryl **3′**. Therefore, the overall barrier for reaction of trisboryl **3′** is lower than that from bisboryl **2′** because the dissociation of borane from **3′** is more favorable than dissociation of borane from **2′** by an energy that is larger than the difference in free energies of activation for the overall C−H bond cleavage and B−C bond forming process from the intermediates resulting from dissociation of borane.

c. Comparison with Other Pathways and Ligand Systems. Recently, theoretical studies on the mechanism of the C−H activation by rhodium boryl complexes similar to those described in this paper were reported.[44] These studies computed pathways involving a trihydride monoboryl complex as the starting species and dissociation of H_2 to generate a boryl hydride intermediate. Our experimental data imply that the monoboryl trihydride complex is not present in the system and that the monoboryl trihydride complex is less thermodynamically stable than either **2** or **3**, but the intermediate generated from the monoboryl complex studied in this previous computational work would, nevertheless, contain one hydride and one boryl ligand, as does the intermediate generated from **2**. The authors concluded that the process occurred by an oxidative addition and reductive elimination pathway, but the presence or absence of an intermediate from oxidative addition on the pathway to C−H bond cleavage and B−C bond formation depended on the computational method. Addition of polarization functions to metal-ligated atoms produced different results.[66] In addition, the computations were conducted with BH_2, not $B(OR)_2$, as the boryl ligand, and this difference in substituent leads to a difference in mechanism, as described below.

The difference in the mechanism for reaction of the hypothetical system with BH_2 as the boryl group[44] and for reaction

Scheme 10

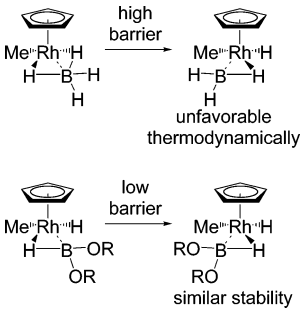

of the current system with a dioxaborolanyl group results from the difference in the barrier for the isomerization. An intermediate with a methyl group trans to the boryl group must isomerize to an intermediate with the methyl group cis to the boryl group for B−C bond formation to occur. The barrier for C−H bond cleavage of methane to generate a product with a hydride cis to the BH_2 group was calculated to be lower than that for C−H bond cleavage to generate a product with a methyl group cis to the BH_2 group. However, the barrier for isomerization of the kinetic addition product to the productive intermediate that contains a methyl group cis to the boryl group was calculated to be too high to occur during the reaction. Because of this high barrier, the authors discounted this pathway and concluded that the reaction occurs by an oxidative addition step that places the methyl group cis to the boryl group.

The barriers for isomerization of the BH_2 and $B(OR)_2$ complexes are different, and the origin of this difference is depicted in Scheme 10. The complex with the hydride cis to a BH_2 group adopts a tetrahydridoborate structure. The strength of the B−H interactions in hydridoborate complexes depends on the substituents at boron. The B−H interaction in a hydridoborate structure with π-donating alkoxide groups on boron is much weaker than the B−H interaction in a hydridoborate structure lacking a π-donor group on boron.[27,46] In fact, the experimental and theoretical studies on the structure of complex **2** imply that there is a significant interaction of the dialkoxyboryl group with only one of the two hydride ligands. As a result of the weak B−H interaction involving a second hydride and a boryl group with alkoxo substituents, the barrier for isomerization of the complex with mutually trans methyl and dialkoxyboryl groups to a complex with mutually cis methyl and dialkoxyboryl groups is low. This low barrier for isomerization allows the product from a low-energy σ-bond metathesis pathway to readily rearrange to an isomer that would form the B−C bond in the final product.

Thus, the choice of boron substituents for the calculation has a large effect on the reaction pathway. Because the experimental work is conducted with dioxaborolanyl groups, and complexes with dialkylboryl ligands do not undergo the C−H activation chemistry,[47] the computational work that is most relevant to the catalytic system is that conducted with dialkoxyboryl ligands.

Conclusion: A New Pathway for C−H Functionalization

Compounds that react through transition-metal boryl complexes are, thus far, unique as small-molecule catalysts for the

(46) (a) Hartwig, J. F.; De Gala, S. R. *J. Am. Chem. Soc.* **1994**, *116*, 3661. (b) Pandey, K. K. *Inorg. Chem.* **2001**, *40*, 5092.
(47) Waltz, K. M.; Hartwig, J. F. *J. Am. Chem. Soc.* **2000**, *122*, 11358.

regiospecific, terminal functionalization of alkanes.[8,48] Further, several catalysts for the functionalization of arenes and benzylic C−H bonds under mild conditions have been reported that react through boryl complexes.[20,31,49] Thus, the reactivity of transition-metal boryl complexes toward C−H bonds is much different from that of transition-metal alkyl or aryl complexes.

Our data suggest that the origin of this difference in reactivity results from a new pathway for the reactions of boryl complexes with the C−H bonds of alkanes and arenes. The computational results imply that the transition-metal boryl complexes cleave the C−H bonds of alkanes with the participation of the boron p-orbital, either directly (as in **17′-TS** or **11b-TS**) or indirectly (as in the changes from **11′-TS** to **13′-TS**). The transition state and product of the C−H bond cleavage process are stabilized by partial B−H bonding. This stabilization by partial X−H bonding would be weaker during the activation of alkanes by metal silyl complexes, and it would be absent during the cleavage of C−H bonds by transition-metal alkyl complexes.

The σ-bond metathesis or [2 + 2] mechanism for the C−H bond cleavage does bear some resemblance to the C−H activation by transition-metal imido and carbene complexes.[3,50,51] Many of these complexes with metal ligand multiple bonds activate hydrocarbons through [2 + 2] pathways,[3,50] and metal boryl complexes are isolobal with metal carbene complexes. Although the metal-to-ligand back-bonding is much weaker in the boryl complexes than in carbenes,[12,52] the orbital interactions during the C−H bond cleavage by boryl and either carbene or imido complexes may be related.

The current work reveals several additional features of the structure and reactivity of metal boryl compounds that contribute to the facility of the catalytic functionalization.

(1) The dissociation of borane from a hydrido boryl complex to generate a 16-electron intermediate occurs under mild conditions. This dissociation is faster than the dissociation of H_2 from the bisboryl dihydride **2** or of B_2pin_2 from the trisboryl monohydride **3**. The dissociation of borane from **2** also occurs much faster than the dissociation of silane from the analogous $Cp^*Rh(H)_2(SiEt_3)_2$.[17]

(2) The structures of the boryl complexes contain some B−H bond character. This partial bonding stabilizes the transition state for C−H bond cleavage, stabilizes the product from C−H bond cleavage, and likely facilitates the dissociation of borane to form the species that undergoes C−H bond cleavage.

(3) The coupling to form a boron−carbon bond is rapid. From the computational studies in this work, the elementary step of B−C bond formation occurs with a low barrier, and previous experimental work on the reactivity of transition-metal boryl complexes implies that this reaction is fast.[53] Because B−C bond formation is rapid, the functionalization process rapidly follows the C−H bond cleavage event. Yet, the computational work suggests that the transition state for B−C bond formation lies slightly above the transition state for C−H bond cleavage.

(4) The alkoxo substituents of the pinacolboryl groups appear to modulate the strength of the B−H interactions. Judging from previous computational work,[44] stable hydridoborate structures are adopted when the B−H interactions between a boryl group and cis hydrides are strong. In this case, the barrier for isomerization becomes large, and the geometry necessary for B−C bond formation is not accessed by the intermediate generated from σ-bond metathesis. Thus, the alkoxo groups create electronic properties that allow for rapid isomerization of the intermediate generated from σ-bond metathesis to a second intermediate that contains mutually cis alkyl and boryl groups.

Overall, our studies on rhodium boryl complexes in the catalytic borylation of alkanes support a mechanism for C−H activation first implied by recent data on stoichiometric reactions of alkanes with iron and tungsten boryl complexes.[10,45,47,54] Two properties that lead to this chemistry in the catalytic borylation of alkanes and arenes are an unoccupied orbital on boron and measurable, but weak, interactions of the boryl ligand with hydrides located cis to them. The formation of a strong B−C bond provides the thermodynamic driving force,[55] and the unoccupied orbital creates fast rates for C−H bond cleavage and formation of the functionalized product.

Experimental Section

General Remarks. All manipulations were conducted under a nitrogen atmosphere using standard Schlenk and glovebox techniques. All NMR spectra were recorded on a Bruker AM-500 NMR spectrometer. ^{1}H NMR chemical shifts are reported in parts per million relative to the peak for residual protiated solvent as an internal reference. ^{11}B NMR chemical shifts are reported relative to the peak for an external standard of $BF_3{\cdot}OEt_2$. Pentane, octane, and cyclohexane were distilled from sodium/benzophenone ketyl prior to use. Benzene-d_6 and toluene-d_8 were dried over sodium/benzophenone ketyl and degassed prior to use. All NMR spectra were recorded using benzene-d_6 as solvent unless otherwise noted. $Cp^*Rh(\eta^4\text{-}C_6Me_6)$[16] was prepared according to literature procedures. B_2pin_2-d_{24} was prepared from BBr_3 as published for the preparation of B_2pin_2,[56] except that the final step of the sequence was conducted with pinacol-d_{12}. The pinacol-d_{12} was prepared by reductive coupling of acetone-d_6 as published for the reductive coupling of acetone.[57] All other chemicals were used as received from commercial suppliers.

Preparation of *trans*-$Cp^*Rh(H)_2(Bpin)_2$ (2). $Cp^*Rh(\eta^4\text{-}C_6Me_6)$ (250 mg, 0.625 mmol) was placed in a 20 mL scintillation vial and

(48) Chen, H.; Hartwig, J. F. *Angew. Chem., Int. Ed.* **1999**, *38*, 3391.
(49) (a) Cho, J. Y.; Tse, M. K.; Holmes, D.; Maleczka, R. E.; Smith, M. R. *Science* **2002**, *295*, 305. (b) Ishiyama, T.; Takagi, J.; Ishida, K.; Miyaura, N.; Anastasi, N.; Hartwig, J. F. *J. Am. Chem. Soc.* **2002**, *124*, 390. (c) Ishiyama, T.; Takagi, J.; Hartwig, J. F.; Miyaura, N. *Angew. Chem., Int. Ed.* **2002**, *41*, 3056. (d) Ishiyama, T.; Nobuta, Y.; Hartwig, J. F.; Miyaura, N. *Chem. Commun.* **2003**, 2924. (e) Ishiyama, T.; Ishida, K.; Takagi, J.; Miyaura, N. *Chem. Lett.* **2001**, 1082.
(50) (a) Slaughter, L. M.; Wolczanski, P. T.; Klinckman, T. R.; Cundari, T. R. *J. Am. Chem. Soc.* **2000**, *122*, 7953. (b) Schafer, D. F.; Wolczanski, P. T. *J. Am. Chem. Soc.* **1998**, *120*, 4881. (c) Schaller, C. P.; Cummins, C. C.; Wolczanski, P. T. *J. Am. Chem. Soc.* **1996**, *118*, 591. (d) Schaller, C. P.; Wolczanski, P. T. *Inorg. Chem.* **1993**, *32*, 131. (e) Cummins, C. C.; Schaller, C. P.; Vanduyne, G. D.; Wolczanski, P. T.; Chan, A. W. E.; Hoffmann, R. *J. Am. Chem. Soc.* **1991**, *113*, 2985. (f) Cummins, C. C.; Baxter, S. M.; Wolczanski, P. D. *J. Am. Chem. Soc.* **1988**, *110*, 8731. (g) Walsh, P. J.; Hollander, F. J.; Bergman, R. G. *J. Am. Chem. Soc.* **1988**, *110*, 8729. (h) Hoyt, H. M.; Michael, F. E.; Bergman, R. G. *J. Am. Chem. Soc.* **2004**, *126*, 1018. (i) Tran, E.; Legzdins, P. *J. Am. Chem. Soc.* **1997**, *119*, 5071. (j) Adams, C. S.; Legzdins, P.; Tran, E. *J. Am. Chem. Soc.* **2000**. (k) Pamplin, C. B.; Legzdins, P. *Acc. Chem. Res.* **2003**, *36*, 223. (l) Wada, K.; Pamplin, C. B.; Legzdins, P.; Patrick, B. O.; Tsyba, I.; Bau, R. *J. Am. Chem. Soc.* **2003**, *125*, 7035.
(51) (a) Debad, J. D.; Legzdins, P.; Lumb, S. A.; Batchelor, R. J.; Einstein, F. W. B. *J. Am. Chem. Soc.* **1995**, *117*, 3288. (b) Adams, C. S.; Legzdins, P.; McNeil, W. S. *Organometallics* **2001**, *20*, 4939. (c) Ng, S. H. K.; Adams, C. S.; Legzdins, P. *J. Am. Chem. Soc.* **2002**, *124*, 9380. (d) Wada, K.; Pamplin, C. B.; Legzdins, P. *J. Am. Chem. Soc.* **2002**, *124*, 9681.
(52) Sakaki, S.; Kai, S.; Sugimoto, M. *Organometallics* **1999**, *18*, 4825.
(53) Rickard, C. E. F.; Roper, W. R.; Williamson, A.; Wright, L. J. *Angew. Chem., Int. Ed.* **1999**, *38*, 1110.
(54) Waltz, K. M.; Muhoro, C. N.; Hartwig, J. F. *Organometallics* **1999**, *18*, 3383.
(55) Rablen, P.; Hartwig, J. F. *J. Am. Chem. Soc.* **1996**, *118*, 4648.
(56) Ishiyama, T.; Murata, M.; Ahiko, T.-H.; Miyaura, N. *Org. Synth.* **2000**, *77*, 176.
(57) Binks, J.; Lloyd, D. J. *J. Chem. Soc. C* **1971**, 2641.

dissolved in dry cyclohexane (5 mL). In a separate vial, HBpin (2.47 g, 19.3 mmol) was dissolved in cyclohexane (5 mL). The two solutions were combined, transferred to a thin wall Pyrex bomb, and sealed under 1 atm of nitrogen. The red solution was irradiated at 10 °C for 24 h, or until the red color of the starting solution had fully disappeared and a clear gold solution was observed. Volatile materials were evaporated under reduced pressure to leave a light tan powder, which was transferred to a sublimation apparatus. Sublimation under dynamic vacuum at 40 °C removed C_6Me_6 and left 274 mg (0.554 mmol, 89%) of a brown powder. The purity of the crude material (>95%)was sufficient for further synthesis. Complex **2** was isolated in pure form as light yellow crystals by the slow evaporation of a pentane solution at −35 °C. Compound **2** is stable under a nitrogen atmosphere at −35 °C for weeks, but slowly decomposes at room temperature. Anal. Calcd for $C_{22}H_{41}B_2O_4Rh$: C, 53.48; H, 8.36. Found: C, 53.21; H, 8.07. ^{1}H NMR: δ 2.04 (s, 15 H, $C_5(CH_3)_5$), 1.13 (s, 24 H, $BO_2C_2(CH_3)_4$), −11.9 (br d, 2H, $^1J_{Rh-H}$ = 40.5 Hz, Rh*H*). ^{13}C NMR: δ 101.6 ($C_5(CH_3)_5$), 82.6 ($BO_2C_2(CH_3)_4$), 25.5 ($BO_2C_2(CH_3)_4$), 11.1 ($C_5(CH_3)_5$). ^{11}B NMR: δ 40.4.

Preparation of Cp*Rh(H)(Bpin)$_3$ (3). Complex **2** (226 mg, 0.457 mmol) was dissolved in neat HBpin (2.57 g, 20.1 mmol). The solution was transferred to a 200 mL glass bomb, sealed under nitrogen, and heated at 105 °C for 3.5 h. The volatile materials were evaporated from the reaction mixture to leave a brown solid. The crude solid was analyzed by ^{1}H NMR spectroscopy and found to contain **3** and **2** in a 5:1 ratio. Following two crystallizations from a pentane solution at −35 °C, 147 mg (0.234 mmol, 51%) of **3** was obtained as light yellow crystals. Compound **3** is stable under a nitrogen atmosphere at −35 °C for weeks but decomposes within hours at room temperature. Microanalysis was not obtained due to the instability of the complex. ^{1}H NMR: δ 2.08 (s, 15 H, $C_5(CH_3)_5$), 1.19 (s, 36 H, $BO_2C_2(CH_3)_4$), −11.3 (br d, 2H, $^1J_{Rh-H}$ = 39.0 Hz, Rh*H*). ^{13}C NMR: δ 102.9 ($C_5(CH_3)_5$), 82.3 ($BO_2C_2(CH_3)_4$), 25.7 ($BO_2C_2(CH_3)_4$), 11.0 ($C_5(CH_3)_5$). ^{11}B NMR: δ 39.9.

Preparation of Cp*RhH(Bpin)P(*p*-C$_6$H$_4$Me)$_3$ (4). Complex **2** (76.1 mg, 0.154 mmol) and P(*p*-$C_6H_4Me)_3$ (46.9 mg, 0.154 mmol) were placed in separate vials and dissolved in equal amounts of C_6H_{12} (2 mL). The solutions were combined in a glass bomb, sealed under nitrogen, and heated at reflux for 4 h. Liberation of HBpin was confirmed by ^{11}B NMR spectroscopy. The volatile materials were evaporated from the reaction mixture to generate a brown oil. Crystallization by slow evaporation of pentane yielded 52.6 mg (0.078 mmol, 51%) of yellow crystals. Anal. Calcd for $C_{37}H_{49}BO_2PRh$: C, 66.38; H, 7.37. Found: C, 66.69; H, 7.67. ^{1}H NMR: δ 7.74 (m, 6H, *p*-$C_6H_4(CH_3)$), 6.98 (m, 6H, *p*-$C_6H_4(CH_3)$), 2.05 (s, 9H, *p*-$C_6H_4(CH_3)$), 1.94 (d, $^1J_{Rh-H}$ = 1.1 Hz, 15H, $C_5(CH_3)_5$), 0.99 (s, 6H, $BO_2C_2(CH_3)_4$), 0.93 (s, 6H, $BO_2C_2(CH_3)_4$), −13.08 (t, $^1J_{Rh-H}$ = $^2J_{P-H}$ = 33.8 Hz, 1H, Rh*H*). ^{13}C NMR: δ 138.7 (d, *p*-C_{aryl}, $^4J_{C-P}$ = 2.1 Hz), 135.2 (d, *ipso*-C_{aryl}, $^1J_{C-P}$ = 46.8 Hz), 134.5 (d, *o*-C_{aryl}, $^2J_{C-P}$ = 11.8 Hz), 128.4 (d, *m*-C_{aryl}, $^3J_{C-P}$ = 10.8 Hz), 98.6 ($C_5(CH_3)_5$), 83.0 ($BO_2C_2(CH_3)_4$), 24.7 ($BO_2C_2(CH_3)_4$), 21.1 ($C_{aryl}CH_3$), 11.0 ($C_5(CH_3)_5$). ^{11}B NMR: δ 42.3 (br). ^{31}P NMR: δ 58.7 (d, $^1J_{Rh-P}$ = 179.1 Hz).

Preparation of Cp*Rh(Bpin)$_2$PEt$_3$ (5). Complex **3** (75.1 mg, 0.120 mmol) and PEt_3 (25.2 mg, 0.213 mmol) were placed in separate vials and dissolved in equal amounts of C_6H_{12} (2 mL). The solutions were transferred to a glass bomb, sealed under nitrogen, and heated at 70 °C for 2 h. Liberation of HBpin was confirmed by ^{11}B NMR spectroscopy. The volatile materials were evaporated from the reaction mixture to leave **5** as a yellow solid. Crystallization from pentane solution at −35 °C yielded 56.4 mg (0.092 mmol, 77%) of yellow crystals. Anal. Calcd for $C_{28}H_{54}B_2O_4PRh$: C, 55.11; H, 8.92. Found: C, 55.08; H, 8.65. ^{1}H NMR: δ 2.06 (s, 15H, $C_5(CH_3)_5$), 1.78 (m, 6H, CH_2), 1.19 (s, 12H, $BO_2C_2(CH_3)_4$), 1.17 (s, 12H, $BO_2C_2(CH_3)_4$), 1.03 (m, 9H, CH_3). ^{13}C NMR: δ 100.0 ($C_5(CH_3)_5$), 81.0 ($BO_2C_2(CH_3)_4$), 26.3 ($BO_2C_2(CH_3)_4$), 25.9 ($BO_2C_2(CH_3)_4$), 19.3 (d, CH_2, $^1J_{C-P}$ = 26.4 Hz), 11.4 ($C_5(CH_3)_5$), 9.1 (CH_3). ^{11}B NMR: δ 42.3 (br). ^{31}P NMR: δ 41.3 (d, $^1J_{Rh-P}$ = 168.8 Hz).

Typical Procedure for the Thermal Reaction of the Boryl Complexes with Hydrocarbons. The metal boryl complexes (5−8 mg) and dodecahydrotriphenylene (3−4 mg) were placed as solids in an NMR sample tube equipped with an airtight valve and were dissolved in 0.5 mL of neat hydrocarbon. Reactions in C_6D_6 were heated at 90 °C, and reactions in alkanes were heated at 125 °C. The reactions were followed by ^{11}B NMR and ^{1}H NMR spectroscopy. Yields of product were determined by either ^{1}H NMR spectroscopy or GC. Response factors for GC measurements were calculated from pure samples of the octyl- and arylboronate esters.

Reaction of 2 and 3 with C$_6$D$_6$ in the Presence of B$_2$pin$_2$-*d*$_{24}$. These experiments were conducted as described for the reactions in the absence of added B_2pin_2-d_{24}, except that B_2pin_2-d_{24} was added prior to the solvent. A typical reaction contained complex **2** or **3** (9−10 mg), B_2pin_2-d_{24} (5−6 mg, 1.1 equiv), and dodecahydrotriphenylene (4−5 mg) in 0.5 mL of neat C_6D_6. The ratio of labeled to unlabeled PhBpin was determined from the areas of the two resolved peaks for PhBpin and PhBpin-d_{12} in the GC trace. The assignments of these two peaks were confirmed by GC/MS.

Reaction of 3 with Added HBpin. The reactions of **3** with benzene and octane in the presence of HBpin were conducted as described for the reactions in the absence of the additive, except that 10 equiv of HBpin was added after the hydrocarbon. The conversion of the starting boryl complex was determined by ^{1}H NMR spectroscopy.

Typical Procedure for the Determination of the Conversion of B$_2$pin$_2$ and Concentration of Rhodium Boryl Complexes. B_2pin_2 (30.3 mg, 0.119 mmol), dodecahydrotriphenylene (11.6 mg, 0.048 mmol), and 16 mol % catalyst were placed in a glass vial and dissolved in pentane (5.0 mL). Most of the solution (4.0 mL) was transferred to a thick-walled glass bomb and sealed under N_2. The remaining solution was divided into two portions for GC and ^{1}H NMR analysis. The bomb was submerged in a circulating oil bath set at the appropriate temperature (Cp*Rh(η^4-C_6Me_6), 125 °C; **2**, 105 °C; **3**, 90 °C). At intervals of 30 min, the bomb was removed from the oil bath and quickly cooled by submersion in an ice−water bath. Two aliquots (∼500 μL) of the solution were removed. The bomb was then resealed under N_2 and placed back into the oil bath. One aliquot was quenched with 10 μL of H_2O, shaken vigorously, and allowed to sit for at least 10 min. This sample was then analyzed by GC, and the conversion of B_2pin_2 was determined by integration of the area of this material versus dodecahydrotriphenylene internal standard. The pentane was evaporated from the second aliquot, and the resulting solid was dissolved in C_6D_6. The quantity of **2** and **3** was determined by ^{1}H NMR spectroscopy by integration of the Cp* signals vs those of dodecahydrotriphenylene.

Reaction of Trisboryl 3 with H$_2$. Complex **3** (7.0 mg) was dissolved in 0.4 mL of C_6D_{12}, and the resulting solution was placed in an NMR tube equipped with a screw cap. The solution was frozen, and the sample tube was evacuated and refilled twice with 1 atm of H_2. The tube was sealed and heated in an oil bath at 40 °C. The ratio of trisboryl **3** to bisboryl **2** was measured by ^{1}H NMR spectroscopy.

General Procedure for Structural Determination by X-ray Diffraction. All data were collected using a Bruker-Nonius KappaCCD diffractometer with graphite-monochromated Mo Kα radiation (λ = 0.71073 Å). The structures were solved by direct methods and refined by full-matrix least squares on F^2 using SHELXTL v. 6.12.[58] Non-hydrogen atoms were refined anisotropically. Hydrogen atoms, with the exception of terminal hydrides, were treated as idealized contributions. Full data collection parameters and structural data are available as Supporting Information.

Computational Details. In the calculations, the pentamethylcyclopentadienyl (Cp*) is modeled by cyclopentadienyl (Cp), and Bpin is truncated to the unsubstituted parent dioxaborolanyl ligand. All

(58) Bruker AXS, Inc., Madison, WI 53719, 2001.

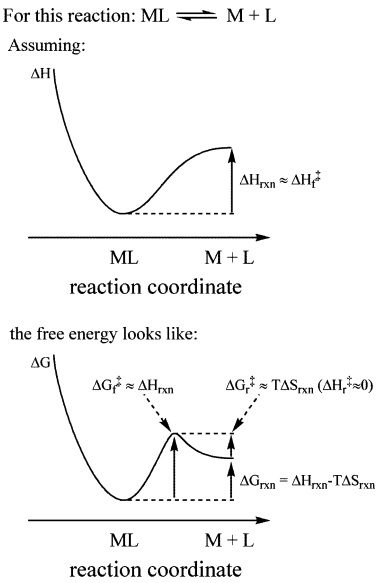

Figure 10. Determination of activation free energies for dissociation and association processes.

calculations have been carried out using the Gaussian 98[40] implementation of B3LYP [Becke three-parameter exchange functional (B3)[59] and the Lee−Yang−Parr correlation functional (LYP)[60]]. A modified version of Hay and Wadt's LANL2DZ[61] was used for rhodium, where the two outermost p functions have been replaced by a reoptimized set, a (41) split.[62] One d polarization and one p diffuse function[63] were added to LANL2DZ[61] for phosphorus. Dunning's cc-pVDZ basis sets[64] were employed for all boron atoms, metal-bound carbons and hydrogens, and all oxygens, while D95[65] was used for all other carbons and hydrogens. All structures were fully optimized, and analytical frequency calculations were performed on each structure to ensure a minimum or transition state was achieved. Zero-point energies were calculated, and thermodynamic functions were computed for 298.15 K and 1 atm, unless otherwise noted. Moreover, the activation free energies for dissociation and association processes were determined as shown in Figure 10.

Acknowledgment. We thank the National Science Foundation for support of this work (Grant Nos. CHE 03-01907, CHE 02-16275, and CHE 98-00184). K.S.C. thanks the NSERC for a postdoctoral fellowship. M.H. thanks the Deutsche Forschungsgemeinschaft (DFG) for a postdoctoral fellowship. Work at Texas A&M University was also supported by The Welch Foundation (Grant A-648). The authors also thank Josiah Manson for a Cerius[2] SDK implementation (in-house code written by J. Manson, TAMU, 2002) of an interface between Cerius[2] and POV-Ray (a ray tracer: POV-Team co/ Hallam Oaks P/L, P.O. Box 407, Williamstown, Victoria, 3016 Australia; http://www.povray.org) used in the production of Figures 3 and 5.

Supporting Information Available: Detailed procedures, data, and CIF files for the structural determination of compounds **2**−**5**. This material is available free of charge via the Internet at http://pubs.acs.org.

JA045090C

(59) Becke, A. D. *J. Chem. Phys.* **1993**, *98*, 5648.
(60) Lee, C.; Yang, W.; Parr, R. G. *Phys. Rev. B* **1988**, *37*, 785.
(61) (a) Hay, P. J.; Wadt, W. R. *J. Chem. Phys.* **1985**, *82*, 270. (b) Wadt, W. R.; Hay, P. J. *J. Chem. Phys.* **1985**, *82*, 299.
(62) Couty, M.; Hall, M. B. *J. Comput. Chem.* **1996**, *17*, 1359.
(63) Check, C. E.; Faust, T. O.; Bailey, J. M.; Wright, B. J.; Gilbert, T. M.; Sunderlin, L. S. *J. Phys. Chem. A* **2001**, *105*, 8111.
(64) (a) Dunning, T. H. *J. Chem. Phys.* **1989**, *90*, 1007. (b) Davidson, E. R. *Chem. Phys. Lett.* **1996**, *260*, 514.
(65) Dunning, T. H.; Hay, P. J. *Modern Theoretical Chemistry, Vol 3: Methods of Electronic Structure Theory*; Schaefer, H. F., III, Ed.; Plenum: New York, 1976; pp 1−28.
(66) For example, addition of polarization functions to metal-ligated atoms for B3LYP calculations makes the geometry of **8** in ref 44 a stable species and drastically changes many of the metric parameters for the MP2 calculated geometries. Fan, Y.; Webster, C. E.; Hall, M. B., unpublished results.